HIGH ENERGY NUCLEUS-NUCLEUS STUDIES AT THE BERKELEY BEVALAC*, **

By L. S. Schroeder

Lawrence Berkeley Laboratory, University of California, Berkeley***

(Received December 21, 1976)

A survey of high energy nucleus-nucleus experiments performed at the Berkeley Bevalac Facility is presented. Experimental results are divided into the general areas of peripheral and central collisions. Results on projectile and target fragmentation, total cross section measurements, pion and photon production, and charged particle multiplicities are stressed. Recently there have been theoretical predictions concerning the possibility of observing new phenomena such as shock waves, pion condensates or collapsed nuclear matter. Existing data relevant to some of these speculations are discussed. A brief discussion of future developments with high energy nuclear beams is also presented.

1. Introduction

In the last few years high energy nuclear beams have become available at several conventional accelerators throughout the world (Berkeley, Dubna, Princeton-Penn, Saclay). With these beams one is able to study high energy nucleus-nucleus collisions at kinetic energies ranging from several hundred to several GeV/nucleon. Recently, high energy deuterons have been accelerated in the CERN PS, and transferred and stored in the ISR [1]. Studies with these high energy nuclear beams provide information in such areas as nuclear and particle physics, astrophysics, cosmic rays, and biology and medicine. In this survey, I will restrict attention to the physical sciences and will discuss only results obtained at the Berkeley Facility [2].

Before proceeding to a discussion of the data, it is useful to list the present experimental parameters which are available at the Bevalac Facility. The Bevalac is a marriage of the SuperHILAC at Berkeley to the Bevatron. The SuperHILAC operates as the injector

* Work done under the auspices of the United States Energy Research and Development Administration.

** Presented at the XVI Cracow School of Theoretical Physics, Zakopane, May 27 — June 7, 1976.

*** Address: Lawrence Berkeley Laboratory, University of California, Berkeley, CA 94720, USA.

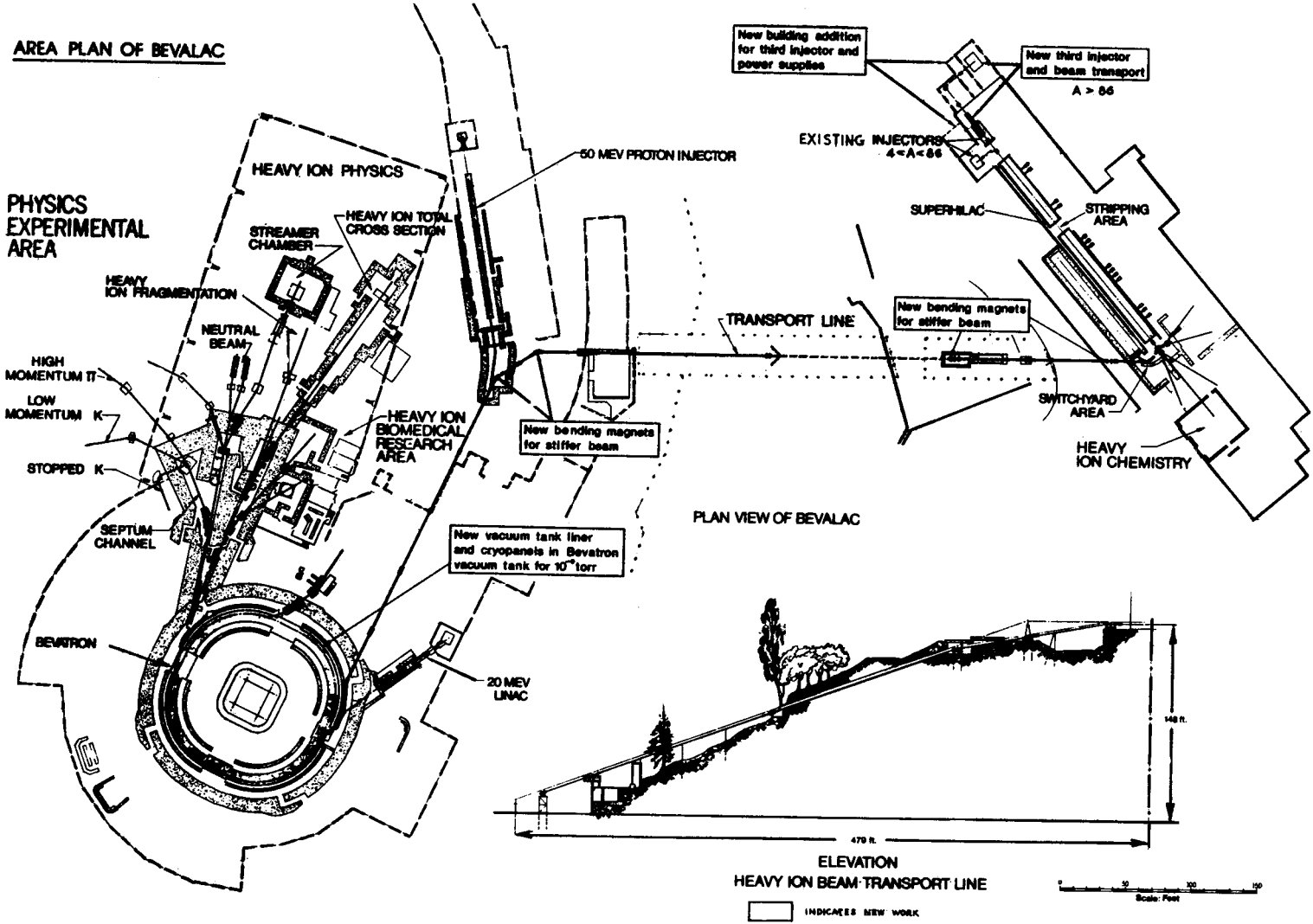
AREA PLAN OF BEVALAC
PHYSICS EXPERIMENTAL AREA
HEAVY ION PHYSICS
STREAMER CHAMBER
HEAVY ION TOTAL CROSS SECTION
HEAVY ION FRAGMENTATION
NEUTRAL BEAM
HIGH MOMENTUM π
LOW MOMENTUM K
STOPPED K
SEPTUM CHANNEL
BEVATRON
HEAVY ION BIOMEDICAL RESEARCH AREA
50 MEV PROTON INJECTOR
New vacuum tank liner and cryopanels in Bevatron vacuum tank for 10⁻⁶ torr
20 MEV LINAC
New bending magnets for stiffer beam
TRANSPORT LINE
New building addition for third injector and power supplies
New third injector and beam transport
A > 86
EXISTING INJECTORS
4<A<86
SUPERHILAC
STRIPPING AREA
New bending magnets for stiffer beam
SWITCHYARD AREA
HEAVY ION CHEMISTRY
PLAN VIEW OF BEVALAC
148 ft.
479 ft.
ELEVATION
HEAVY ION BEAM TRANSPORT LINE
INDICATES NEW WORK
Scale: Feet

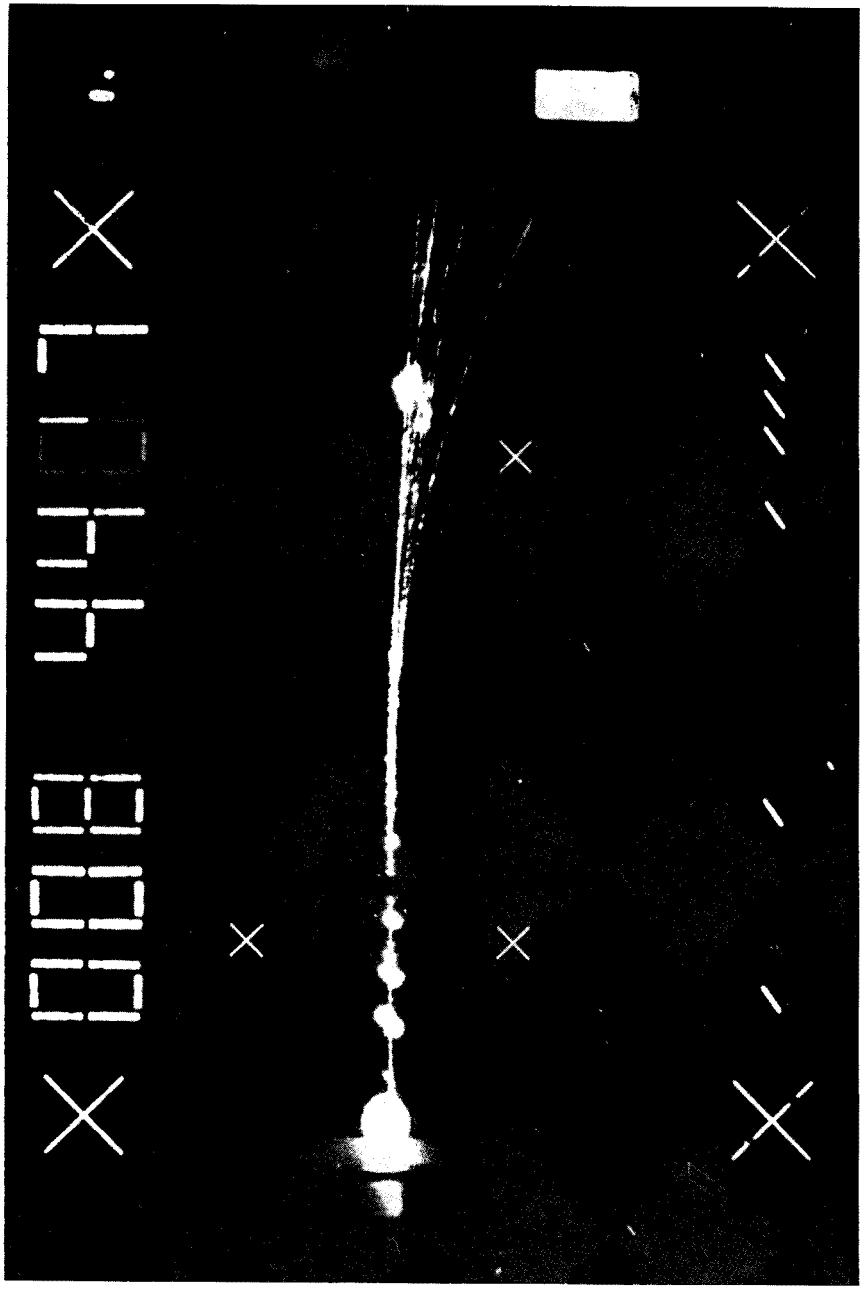

Fig. 2. Fragmentation of 0.87 GeV/nucleon ^{12}C projectile on lucite target located inside LBL streamer chamber. Six charged particles are visible

of heavy ions at 8.5 MeV/nucleon into the Bevatron. Once in the Bevatron, the beam is accelerated and extracted into the experimental hall. Energies of the ions can be continuously varied from 0.2 — 2.5 GeV/nucleon (kinetic energy/nucleon).

Figure 1 shows a plan view of the SuperHILAC/Bevatron complex. Note that the SuperHILAC is actually about 150 feet higher in elevation than the Bevatron. Table I lists the ions available along with expected beam intensities.

TABLE I

Types and fluxes of heavy ions at Bevalac facility

Ion	Particles/Pulse
^{1}H	4×10^{12}
^{2}H	2×10^{11}
^{4}He	2×10^{10}
^{12}C	3×10^{10}
^{14}N	3×10^{10}
^{16}O	3×10^{10}
^{20}Ne	10^{10}
^{40}Ar	4×10^{8}
^{56}Fe	5×10^{5}
^{84}Kr	4×10^{4}

At present, beams up to Ar are routinely available for experiments and recently ^{56}Fe was accelerated and extracted for experiments for the first time.

The experimental results that will be discussed are from experiments that have been performed at the Bevalac over the last few years. Where appropriate, results from other accelerators will be quoted. To facilitate the discussion of experimental results, I have broken the studies into two broad classifications: *peripheral* and *central* collisions. Although this is a convenient division for this talk, it must be remembered that any particular reaction can fall into either or both of these areas, depending on the kinematical region being studied. When discussing a particular experiment, I will attempt to include the following information: motivation for experiment, detection techniques, experimental results, possible interpretation of results, and summary.

2. *Peripheral collisions*

There are four topics which will be discussed under this general area: they include projectile fragmentation, pion production, heavy ion total cross sections, and gamma-ray production.

A) Projectile Fragmentation: Before turning to a discussion of specific experiments, let us first characterize the process of projectile fragmentation. It requires relatively little energy transfer (little, compared to the incident projectile energy) to breakup a nucleus.

We then expect that the following picture would result:

The characteristic angle of emission of these fast projectile fragments would essentially be determined by the transverse Fermi mometum/nucleon in the incident nucleus and the longitudinal momentum/nucleon of the projectile. For example, a 2.1 GeV/nucleon incident projectile has a longitudinal momentum/nucleon, p, of 2.89 GeV/c. Using an average Fermi momentum/nucleon of = 100 MeV/c, we have:

$$\langle \sin \theta_{\text{frag}} \rangle = \frac{p_{\text{T}}}{p} = \frac{0.1}{2.89} = 0.035$$

or,

$$\langle \theta_{\text{frag}} \rangle \approx \langle \sin \theta_{\text{frag}} \rangle \approx 2.7°.$$

So, we expect the particles emitted in projectile fragmentation processes, to be moving fast and highly collimated in the laboratory. Fig. 2 shows an example of the fragmentation of an 0.89 GeV/nucleon ^{12}C beam in the LBL streamer chamber [3] In this picture, six charged tracks are seen emerging from the interaction region (a lucite target located in the chamber at the position of the *apparent* break of the incident track) and are tightly bunched in a narrow cone around the beam direction. Thus, the process of projectile fragmentation is one which can be used to study the nucleus and its structure under the condition of small energy and momentum transfers.

When discussing some of the experimental results, it will be useful to use the parameter, y, which represents the rapidity of a particle. The rapidity is defined by: $y = 1/2 \ln([E+P_{\|}]/[E-P_{\|}])$, where E is the energy of the detected particle and $P_{\|}$ its longitudinal momentum. The rapidity of a 2.1 GeV/nucleon projectile is about 1.8 units. Therefore, we expect that in the projectile fragmentation process, fragments will emerge with rapidities near the beam rapidity and at small emission angles. This should be compared to the case of target fragmentation, where the fragments are emitted slow ($y_{\text{frag}} \approx 0$) and essentially isotropically in the laboratory frame. Whereas many of the traditional techniques of high energy physics lend themselves to studying projectile fragmentation: low energy nuclear physics techniques are best suited to detection of the target fragmentation process.

One of the first systematic studies of projectile fragmentation was performed by Heckman et al. [4]. This group has been studying single-particle inclusive distributions near 0° at projectile energies of 1.05 and 2.1 GeV/nucleon. That is, they have studied: $A+B \rightarrow C+x$ at $\theta_{\text{Lab}} \approx 0°$, where the incident projectile A has been ^{12}C, ^{14}N, ^{16}O, ^{20}Ne, and ^{40}Ar, and B the target nucleus has been varied over the full range of the periodic table. C represents the single fragment detected by their apparatus. The motivation for

this work has come from three different areas: nuclear structure, particle physics, and cosmic rays. In the area of nuclear structure it was felt that the projectile fragmentation process would necessarily bias one towards low energy transfer processes. In such processes, individual nuclear clusters would be emitted into a small angular cone in the forward direction. A measurement of the single particle momentum spectrum would then perhaps serve as a means of measuring the internal momentum distribution of particles inside the projectile before the fragmentation occurred. In effect, providing a "snap-shot" of the projectile nucleus before the interaction. The second area of interest concerns the usefulness of such data in the area of high energy physics. Certainly, nuclei clearly exhibit

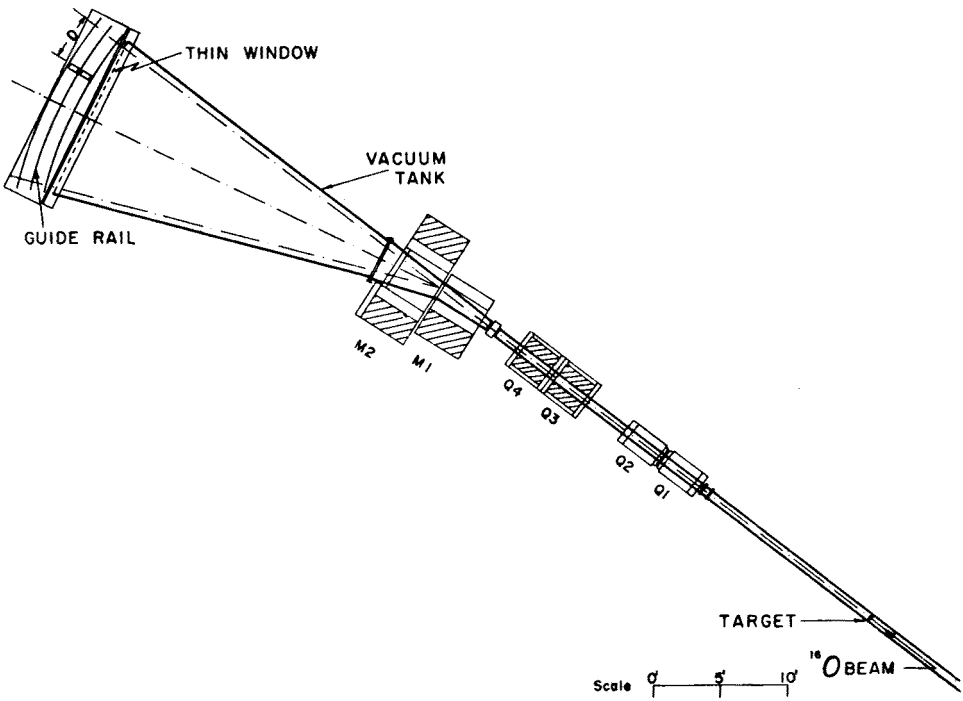

Fig. 3. Plan view of magnetic spectrometer used to study projectile fragmentation near 0°

a "constituent" nature, since they are composed of nucleons. It is then interesting to apply Glauber-type models to an understanding of the fragmentation process. Also at energies of 1 — 2 GeV/nucleon, target and projectile fragmentation regions should be well separated. If one can establish a clear separation of the fragmentation regions, then it is tempting to determine to what extent the concepts of scaling and limiting fragmentation can be applied to these nuclear processes. Indeed, perhaps these concepts can be applied at much lower energies for some nuclear processes than their elementary particle counter parts. Finally, a knowledge of fragmentation cross sections plays a vital role in the understanding of the propagation of cosmic rays from their source. Thus, these measurements become extremely useful for astrophysical purposes.

Fig. 3 shows a plan view of the spectrometer used to study projectile fragmentation. Detectors consisting of plastic scintillators, solid-state counters and multi-wire chambers were placed at the end of the vacuum tank. The individual fragments produced near 0° were identified (mass and charge) using a combination of rigidity (momentum/unit charge), time-of-flight and energy loss (dE/dX). Two types of measurements have been made by

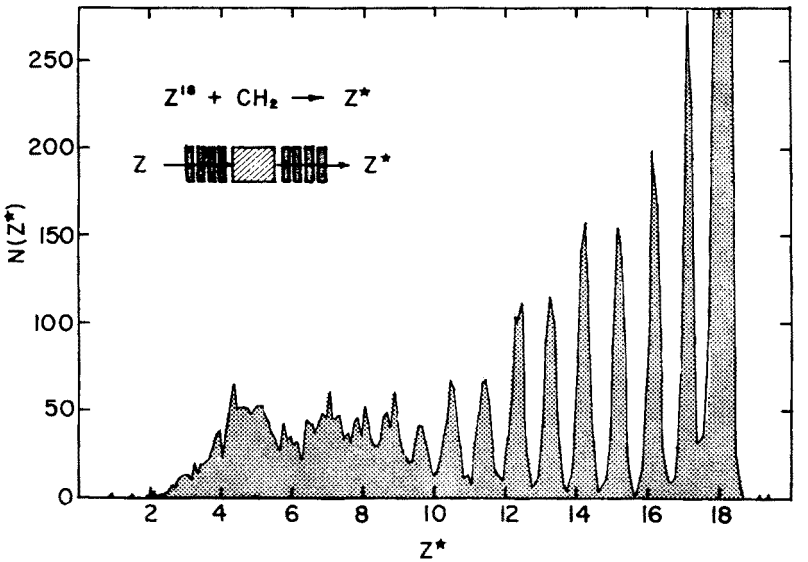

Fig. 4. Fragmentation of ^{40}Ar beam into different final charge states

his group. The first method consists of measuring the cross section for the fragmentation of the projectile into various charges. In Fig. 4 is shown a typical charge spectrum that results when ^{40}Ar ($Z = 18$) bombards a CH_2 target. The experiment measures the incident charge Z and the "effective" outgoing charge $Z^* = (\sum_i Z_i^2)^{1/2}$ For the example shown, it is clear that a large amount of the cross section goes into the production of one large charge (e.g. $Z \simeq 12-17$) in association with one or more smaller charges. However, note that a substantial fraction of the cross section is involved with much less charge out than was present in the beam. This is partly due to the geometry of the apparatus, but also reflects the fact that there can be collisions in which very few particles go forward so that most of the available charge is emitted into angles outside their detector. This means that there were many particles produced in such collisions and that these probably represent a more central collision. This point should be remembered when we come to a discussion of central collisions.

Now let us consider some of the results that have been obtained in their studies of projectile fragmentation near 0°. In these experiments, a single fragment is detected and identified. Both target and projectile have been varied for these studies. However, the general features (e.g. momentum spectra) they have studied are found to depend very little on the detailed nature of the target or the projectile. Fig. 5 shows a typical momentum

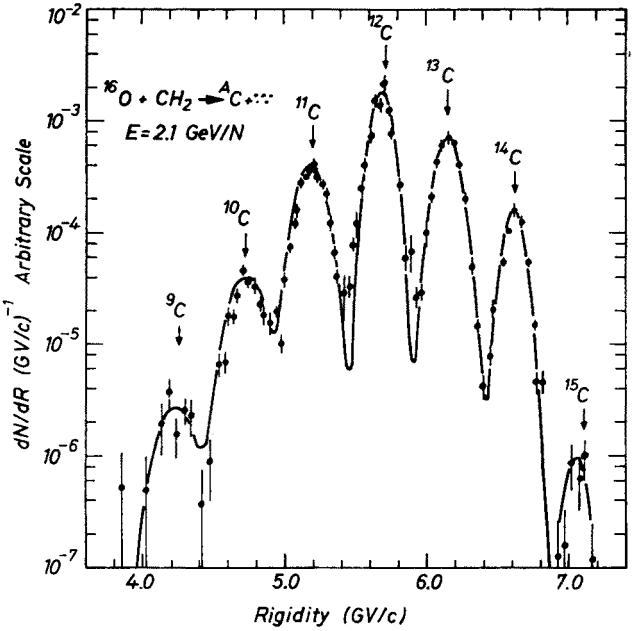

Fig. 5. Data of Ref. [4] showing the fragmentation of an ^{16}O beam at 2.1 GeV/nucleon into carbon isotopes. Cross section (arbitrary units) versus momentum/unit charge (rigidity)

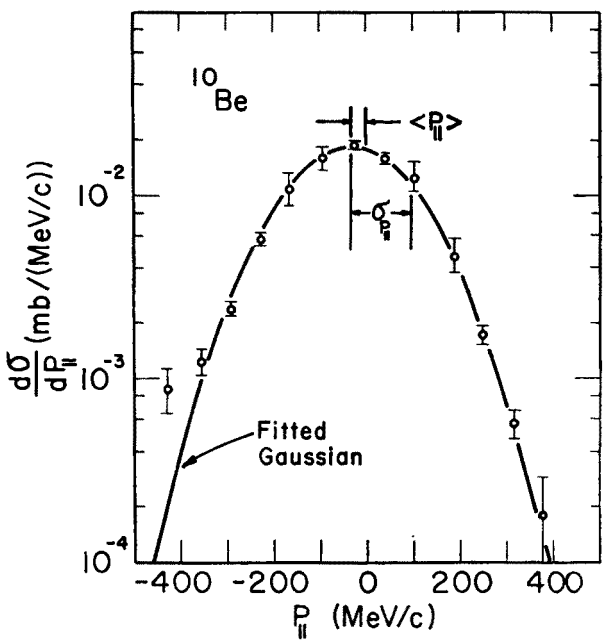

Fig. 6. Data of Ref. [4] on the fragmentation process $^{12}C + Be \rightarrow {}^{10}Be + x$ at 2.1 GeV/nucleon. Cross section versus longitudinal momentum in the projectile rest frame

spectrum for the fragmentation of a 2.1 GeV/nucleon ^{16}O beam into carbon isotopes. The cross section (in arbitrary units) is plotted against the rigidity (p/Z). A number of peaks appear which can be identified as due to specific carbon isotopes. If one transforms any one of these distributions into the rest frame of the projectile, it is found to be gaussian in shape, and peaked near zero momentum in that frame. Fig. 6 shows such a distribution, this time for the fragmentation of a 2.1 GeV/nucleon ^{12}C projectile into ^{10}Be. Again, these general characteristics are relatively independent of projectile and target. This result was not anticipated and at first was without an adequate explanation.

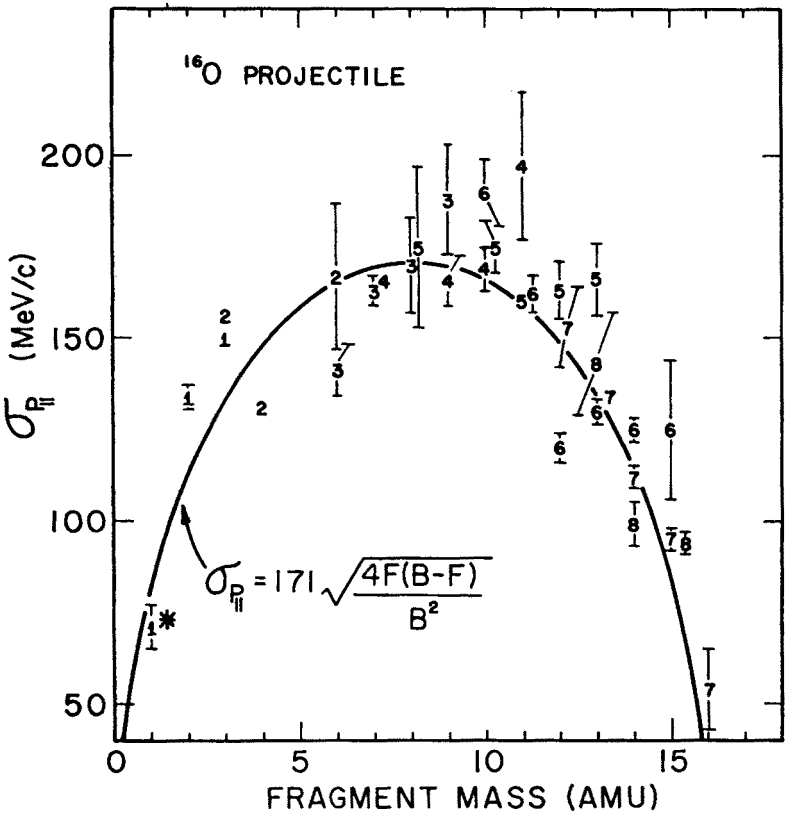

Fig. 7. Target averaged width, $\sigma_{p_\parallel}$ of the projectile frame longitudinal momentum distribution (MeV/c) versus observed fragment mass for a 2.1 GeV/nucleon ^{16}O beam. Data from Ref. [4]

From these single-particle inclusive studies [4] the following conclusions can be made:

1) For the majority of detected fragments, they observe that the single-particle momentum distributions are gaussian in shape and are peaked near zero momentum in the projectile rest frame. These distributions can be parameterized in the projectile rest frame as:

$$\frac{d^3\sigma}{dp^3} = ce^{-(p_T^2/2\sigma_T^2)}e^{-((p_\parallel - \langle p_\parallel \rangle)^2/2\sigma_\parallel^2)},$$

where p_T and $p_\parallel$ are the transverse and longitudinal momentum of the fragment, $\langle p_\parallel \rangle$ is the value of the off-set from zero momentum (see Fig. 6), and σ_T and $\sigma_\parallel$ are the FWHM for the transverse and longitudinal momentum distributions. Within their estimated errors of $\pm 10\%$, they find that $\sigma_T = \sigma_\parallel$.

2) They have investigated the dependence of the gaussian momentum distributions on the masses of the fragment F, and the mass of the projectile, B, averaged over target material. In Fig. 7 is shown a plot of $\sigma_\parallel$ (the FWHM for the longitudinal momentum distribution) versus the mass of the fragment for the fragmentation of an ^{16}O beam. The parabolic curve is from a theoretical calculation [5] which employed a "sudden-approximation" along with shell-model wave functions. The data points are seen to generally follow this parabolic behavior, which is given by:

$$\sigma_\parallel^2 \propto \frac{F(B-F)}{B^2}. \tag{1}$$

The parabolic dependence of $\sigma_\parallel^2$ on fragment mass was first predicted by Wenzel [6] later by Lepore and Riddell [5] and indirectly by Feshbach and Huang [7] as extended by Goldhaber [8]. The parabolic shapes arise when one assumes:

(a) Fragment momentum distributions are essentially those in the projectile nucleus.

(b) There are no correlations between the momenta of different nucleons, and

(c) Momentum is conserved.

3) The dependence of the fragmentation cross section is found to factor into target and projectile related parts. If we write the reaction as, $A+B \rightarrow C+X$, then this factorization can be expressed as: $\sigma_{AB}^C = \gamma_A^C \gamma_B$, where γ_A^C depends only on the projectile and the detected fragment, and γ_B depends only on the target material. They have found that $\gamma_B \propto B^{1/4}$ suggesting a peripheral interaction. It is also possible to parameterize the cross section as $\gamma_B \propto (A^{1/3}+B^{1/3}-\varepsilon)$, where ε plays the role of an overlap parameter.

There have been a number of theoretical models which have attempted to predict some of the regularities that have been observed for the process of projectile fragmentation. Feshbach and Huang [7] have used a statistical model in association with "virtual clusters" to explain the earlier data. A. Goldhaber [8] showed that a thermodynamic model could be used to explain the parabolic shape of $\sigma_\parallel^2$. Lepore and Riddell [5] employed a quantum mechanical model using the sudden approximation and shell-model wave functions to explain the gaussian momentum distributions and the parabolic dependence of $\sigma_\parallel^2$. Recently Hüfner and collaborators [9] have extended and abrasion-ablation model originally proposed by Bowman et al. [10]. In this model, the fragmentation process takes place in two stages. In the first, the abrasion stage, the overlapping nuclear matter is sheared away from the projectile and target. The remaining pre-fragment has a recoil momentum proportional to the Fermi momentum [9]. This pre-fragment is left in an excited state and subsequents decays into nucleons and/or nuclear clusters, which is the ablation stage. It is one of these fragments which is detected. Hüfner et al. [9] use a Glauber-model to treat the first or abrasion stage. For the ablation stage they assume thermalization of the pre-fragment and compound nucleus decay. Both these assumptions remain to be proven, but they at least allow the calculation to be done. Their two-step model reproduces

the overall trend of the existing data on projectile fragmentation and the isotopic dependence for the widths of the experimental momentum distributions. However, they find that $\sigma_{\parallel} \neq \sigma_T$, but differs by about 5–10%, which is of the size of the quoted experimental errors. This model appears to provide a step forward in our understanding of the fragmentation process. However, it is evident, that much more theoretical work is required. Also more complicated experiments will be required to distinguish between some of the models being proposed.

An additional interesting feature of these data has been observed for the case where a single nucleon is removed from the incident projectile [11]. An example of this being, ^{16}O fragmenting to ^{15}O (neutron removal) or ^{15}N (proton removal). Figure 8 shows the

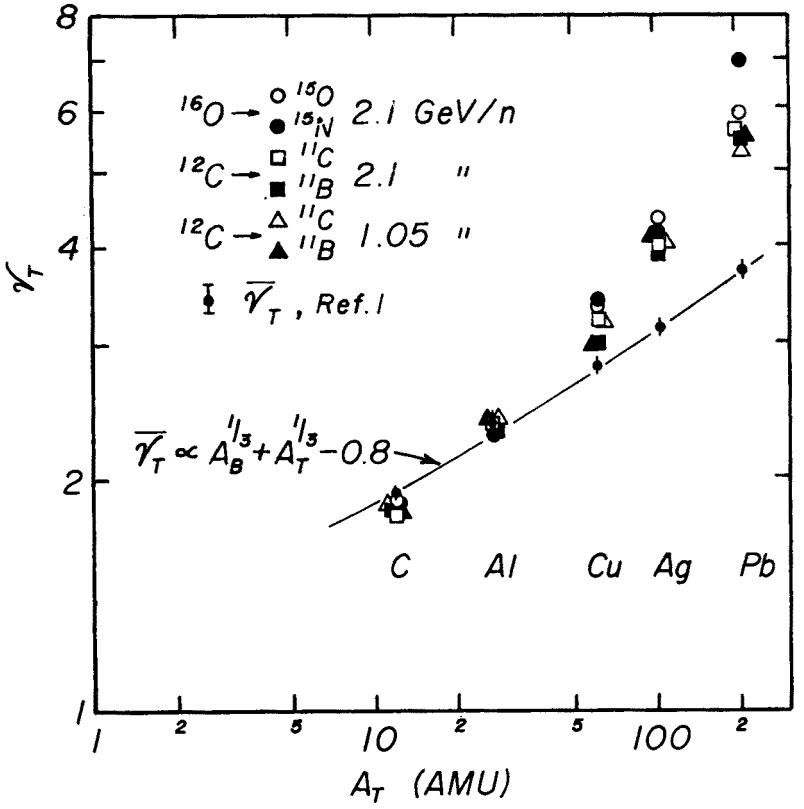

Fig. 8. Target factor γ_T versus target mass. Data are for single nucleon removal reactions involving ^{16}O and ^{12}C beams at 1.05 and 2.1 GeV/nucleon

target factor, γ_T, plotted against the mass of the target. The data shown are just for the single nucleon removal reactions. The solid curve ($\bar{\gamma}_T$) represents the behavior for all other fragmentation processes. The single nucleon removal data is seen to follow this trend for light targets (up to about Al), but shows strong deviations for heavier targets which are found to be proportional to Z^2, suggesting that coulomb dissociation plays

a major role. A simple model using the Weizsacker-Williams approximation was constructed to explain the single nucleon removal data. In this model, the cross section for single nucleon removal is assumed to go as:

$$\sigma_{WW} = \int \sigma(\omega) N(\omega) d\omega, \tag{2}$$

where σ_{WW} is the cross section of interest, $\sigma(\omega)$ is the photo-nuclear cross section as a function of photon frequency ω, and $N(\omega)$ is the density of photons obtained by using the Weizsacker-Williams techniques. Figure 9 shows the results of their calculation

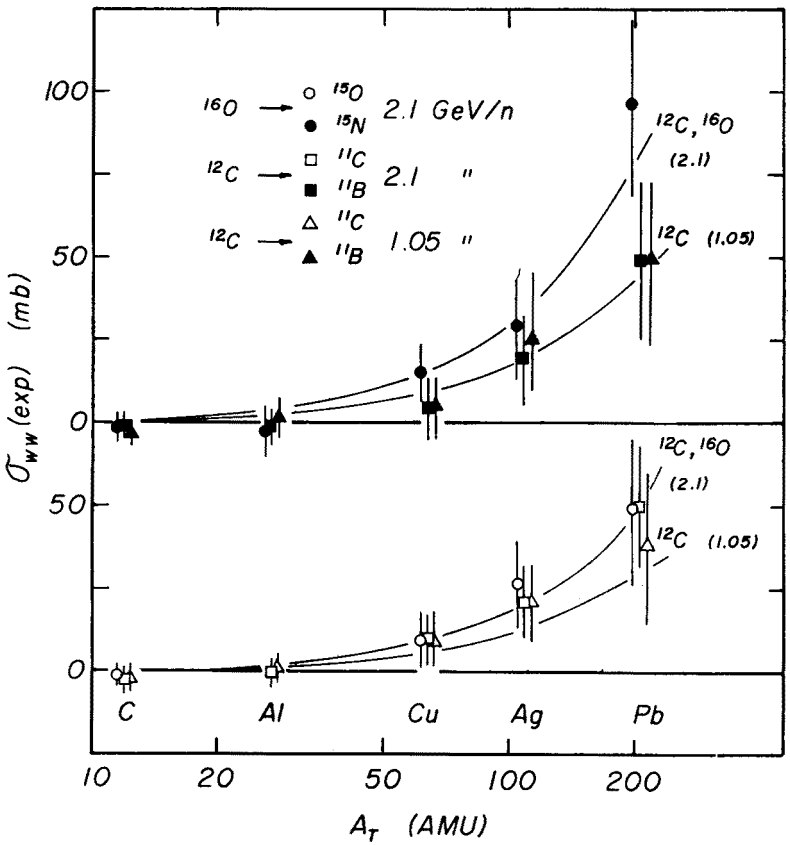

Fig. 9. Experimental data of Ref. [11] for single nucleon removal reactions compared to results of model calculation using coulomb dissociation

compared to the data. The data and the model are in excellent agreement. Thus, both nuclear and coulomb forces are seen to play major roles in projectile fragmentation processes [9,11].

Up to this point we have considered the fragmentation of incident beams with $A \geqslant 12$. We now consider some results from a study of light-ion (d, α, C) fragmentation by Papp et al. [12]. This experiment measured the single particle inclusive spectra of particles at

$\theta_{Lab} = 2.5°$, produced in the collision of 1.0–4.2 GeV protons, 1.05 and 2.1 GeV/nucleon deuterons and alphas, and 1.05 GeV/nucleon carbon beams with a variety of nuclear target (Be, C, Cu, Pb). Emphasis was placed on the detection of protons, deuterons, tritons, ^{3}He, and ^{4}He using a combination of magnetic rigidity, dE/dx, and time-of-flight measurements with plastic scintillators as detectors. This group was interested in examining the connection between the observed momentum spectra of projectile fragments and the internal momentum distributions of these particles inside the nucleus. In addition, these

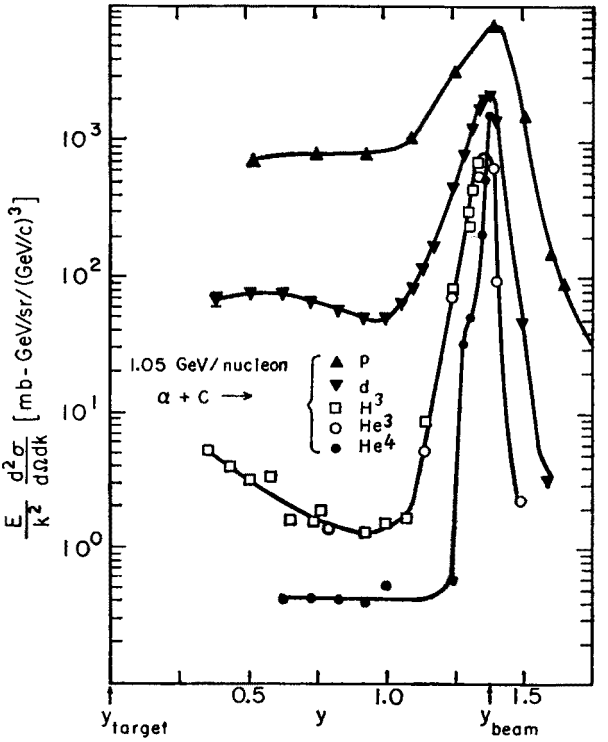

Fig. 10. Data of Ref. [12] for the fragmentation of 1.05 GeV/nucleon alphas by a carbon target. Individual fragments, detected at $\theta_{Lab} = 2.5°$, are indicated

distributions were studied for their dependence on target material and incident energy. Finally, they were interested in seeing if the concepts of limiting fragmentation and scaling would apply to these light-ion fragmentation processes.

Data for the production of light nuclei at 2.5° (Lab) by 1.05 GeV/nucleon alphas is shown in Fig. 10. The Lorentz invariant cross section,

$$E/k^2\left(\frac{d^2\sigma}{d\Omega dk}\right)$$

is plotted versus the repidity (y) of the detected fragment. These data were taken with a carbon target. Substantial peaks are observed for each of the fragment distributions shown. These peaks are centered at the rapidity of the beam, a result consistent with the

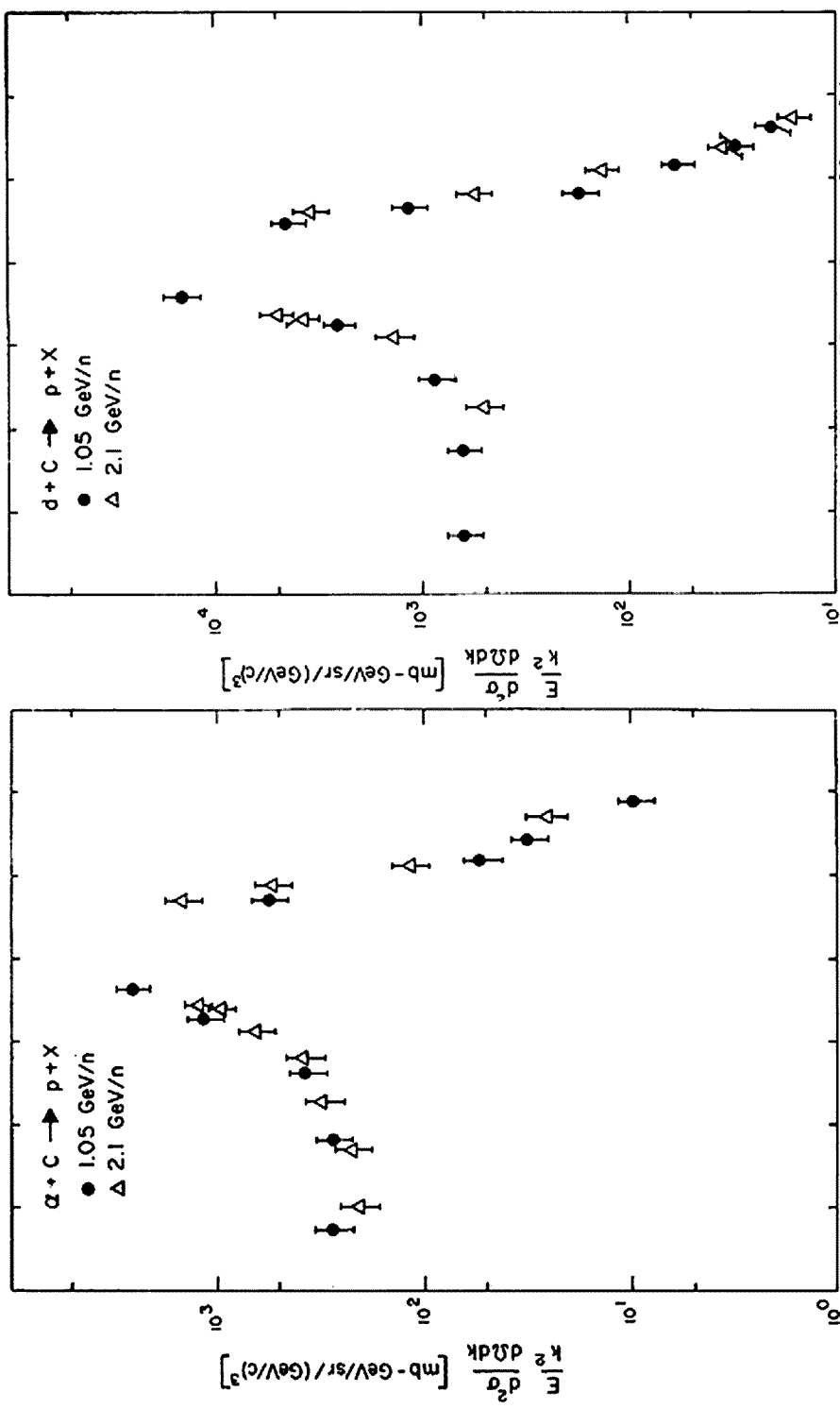

Fig. 11a, b. Lorentz invariant cross section for (a) deuteron or (b) alpha beam fragmenting to a proton versus the proton momentum. Incident energies are 1.05 and 2.1 GeV/nucleon

finding of Heckman et al. [4] in their fragmentation studies. Also from Fig. 10 we can see that there is a clear separation between the projectile ($y \simeq y_{\text{beam}}$) and target ($y \simeq 0$) fragmentation regions. Also note that for those cases where there exists overlapping data points, the ^{3}H and ^{3}He production cross sections agree reasonably well as expected for particles from the same iso-spin multiple.

Since target and projectile fragmentation regions are well separated, can we expect that limiting fragmentation might hold? If limiting fragmentation is valid for nuclear fragmentation processes, it is expected to be independent of energy and target material in this experiment. It was observed that the shapes of the momentum spectra were independent of the target used in the region of the projectile fragmentation peaks [12]. This was also observed by Heckman et al. [4] in their studies with heavier beams. The question of the energy dependence of the fragmentation peaks is complicated by the fact that these measurements were made at a fixed laboratory angle (2.5°), and therefore sample a range of transverse momenta. To test limiting fragmentation, one needs to compare cross sections for processes like $d+A \rightarrow p+x$, where A is some nucleus, in the region of the proton fragmentation peaks at 1.05 and 2.1 GeV/nucleon. Being at fixed laboratory detection angle means that the transverse momenta at these peaks are not the same. The next best thing that can be done is to make a comparison at the same value of the overall momentum ($p = \sqrt{p_{\parallel}^2+p_{\text{T}}^2}$) in the projectile rest frame. Fig. 11 (a, b) shows the invariant cross sections at 1.05 and 2.1 GeV/nucleon for the processes $dC \rightarrow p+x$ and $\alpha C \rightarrow p+x$, versus the momentum (p) of the proton in the *projectile rest frame*. Lack of data at $p \approx 0$, reflects the fact that the measurements were made at a fixed laboratory angle. The data are consistent (within the errors) with an energy independence for these processes at 1.05 and 2.1 GeV/nucleon. This result is not undeniable proof of the validity of limiting fragmentation for these processes, but is certainly consistent with the concept. More detailed measurements at fixed p_{T} are required to shed more light on this intriguing possibility.

Further insight on the production mechanism for particles can be obtained by studying the dependence of the production cross section on target mass. The data have been parametrized in the form $\sigma \propto A^n$, where A is the atomic mass of the target, and n is obtained from a fit to the data. Figure 12 shows a plot of the coefficient n versus the momentum of the proton for the two processes, $dA \rightarrow p+x$ and $\alpha A \rightarrow p+x$ at 2.1 GeV/nucleon. For high momentum the cross section varies at $A^{1/3}$, suggesting that the fragmentation process is peripheral. For lower momentum the cross section shows rapid growth, perhaps suggesting a more central collision.

Before turning to pion production, it is worth summarizing the bulk of the existing data on projectile fragmentation:

1) Primarily a peripheral (surface) process which dominates the cross section for particle production at forward angles and high momenta.
2) Fragments are produced near the beam's rapidity.
3) Limiting fragmentation appears to be a valid concept for certain nuclear processes, such as $\alpha A \rightarrow p+x$.
4) Other processes contribute at forward angles besides projection fragmentation.

B) Pion Production: In addition to light-ion fragmentation studies, Papp et al. [13] have also studied pion production. The experiment was a single particle inclusive study of:

$$\begin{pmatrix} p \\ d \\ \alpha \\ C \end{pmatrix} + A \rightarrow \pi^{\pm} + x \quad \text{at} \quad \theta_{\text{lab}} = 2.5°.$$

This experiment measured the single pion inclusive spectra produced by high energy proton, deuteron, alpha and carbon beams interacting with a variety of targets (Be, C, Cu, Pb). A primary goal for these experiments was to determine to what extent very energetic

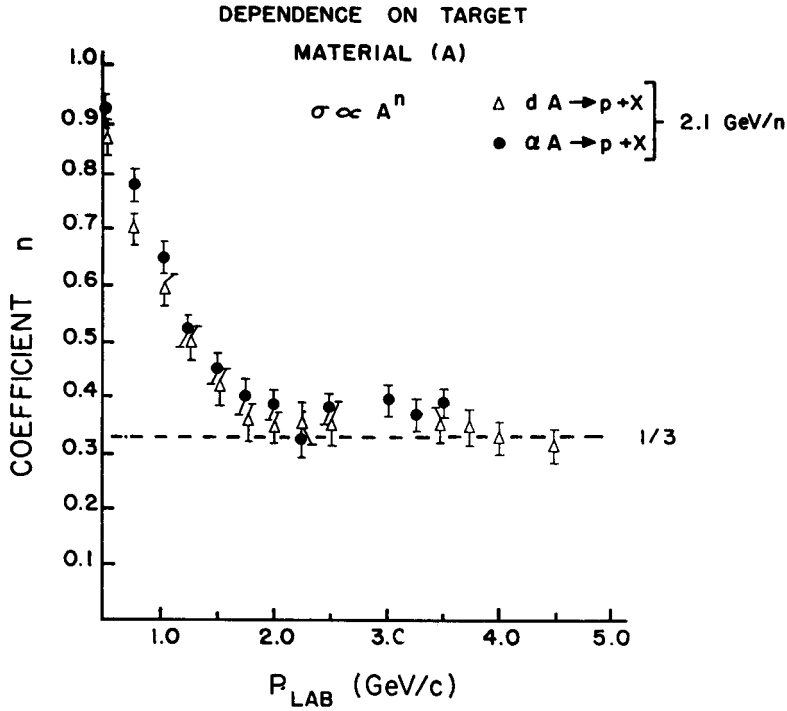

Fig. 12. Dependence of deuteron and alpha beam fragmentation to protons on target mass at 2.1 GeV/nucleon. Data for various targets was fit (least squares) to the form: $\sigma \propto A^n$, A = mass of target

pions, that is, pions with energies considerably larger than those which result from simple nucleon-nucleus collisions, are produced in the collisions of deuteron, alpha and heavier beams with nuclei. Could such high energy pions be explained in terms of nucleon-nucleon processes in which Fermi motion is included in both projectile and target, or are more complicated processes such as some cooperative phenomena involved? Such data can also be used to test whether high energy ideas such as scaling [14] can be applied to pion production resulting from nuclear collisions.

Figure 13 shows the result of π^- production by 1.05–4.8 GeV protons on a carbon target. The spectra are observed to fall rapidly at higher pion momenta. The sharp cut-off in each spectrum is a result of energy and momentum conservation and corresponds to the proton transferring almost all its kinetic energy to the creation of a pion. A remarkable

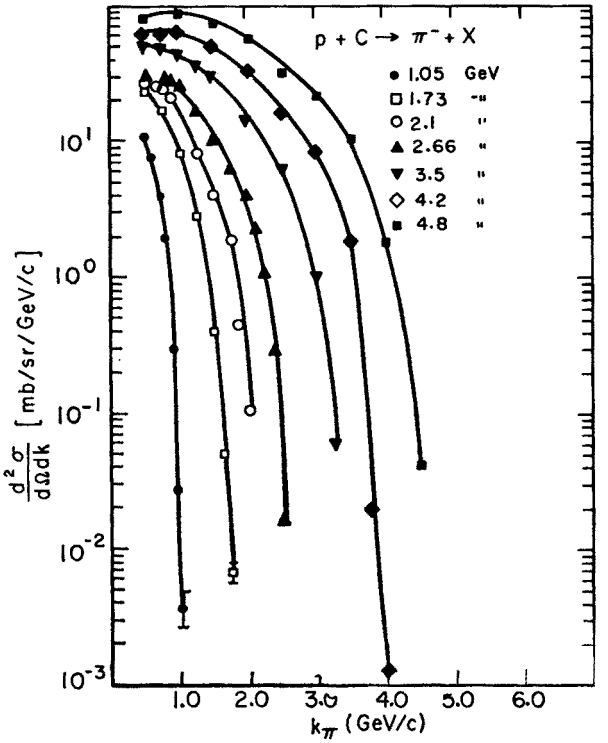

Fig. 13. Cross section for negative pion production at 2.5° (lab.) by 1.05 to 4.8 GeV protons from a carbon target versus the pion momentum, k_π

feature of these data is observed when the invariant cross section $E/k^2(d^2\sigma/d\Omega dk)$ is plotted against the scaling parameter,

$$x' = \frac{k_{\parallel}^*}{(k_{\parallel}^*)_{\max}} \text{ as shown in Fig. 14a.}$$

All the data are seen to lie on a universal curve, suggesting that negative inclusive pion spectra scale even at 1 GeV, a somewhat unexpected result. A similar feature is observed for each of the target nuclei used. This scaling behavior, where the pion yield does not depend on the energy but only on the scaling parameter x' (at fixed $k_\perp$) is familiar in very high energy elementary particle processes. It must be remembered that this experiment was performed at a fixed lab angle of 2.5°, so that $k_\perp$ was not quite constant. This effect [13] is most important near $x' = 1$ where it could change the results by as much as a factor

of 2. Figure 14b shows the invariant cross section for producing negative pions by 1.05 and 2.1 GeV/nucleon deuteron and alpha projectiles on a carbon target. Again the scaling feature is reasonably satisfied. Notice that the fall off in x' increases at the mass of the incident projectile increases. This suggests that relatively loosely bound objects, like nuclei,

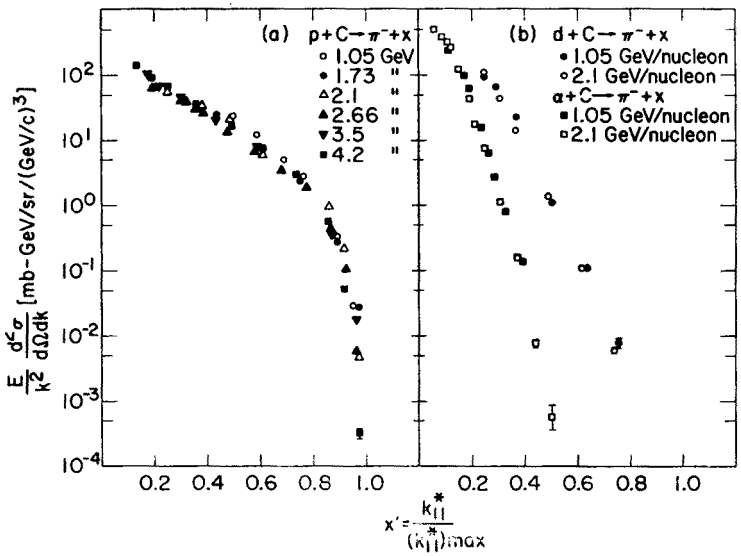

Fig. 14a, b. Invariant cross section (Ref. [13]) for negative pion production at 2.5° (Lab) (a) incident protons (1.05–4.2 GeV), (b) incident deuterons and alphas (1.05–2.1 GeV/nucleon)

do not transfer a large fraction of their kinetic energy to creating individual pions. For the case of π^- production by deuterons, these results differ from those of the Dubna group [15] who find that the ratio:

$$R(x') = \frac{\sigma(\mathrm{d}+\mathrm{Cu} \to \pi^- + x)}{\sigma(\mathrm{p}+\mathrm{Cu} \to \pi^- + x)}$$

at the same total kinetic energy is independent of x' in the interval $0.6 \lesssim x' \lesssim 1.0$.

Negative pion production cross section [13] for 2.1 GeV/nucleon proton, deuteron, and alphas incident on a carbon target are shown in Fig. 15. The following features are evident:

1) The heavier the projectile, the larger the cross section (at 1 GeV/c this ratio is $\sim 10:5:1$),

2) The maximum energy of observed pions increases as the mass of the projectile increases.

The larger production cross sections for deuterons and alphas compared to protons is attributed to the presence of neutrons which produce π^-'s more abundantly than do protons.

It is of considerable interest to ascertain whether these high energy pions are produced in interactions in which several nucleons inside the projectile nucleus participate in a cooperative fashion, or whether a single nucleon-nucleus collision with the inclusion of Fermi motion in both projectile and target is sufficient to explain the observed spectra. A simpli-

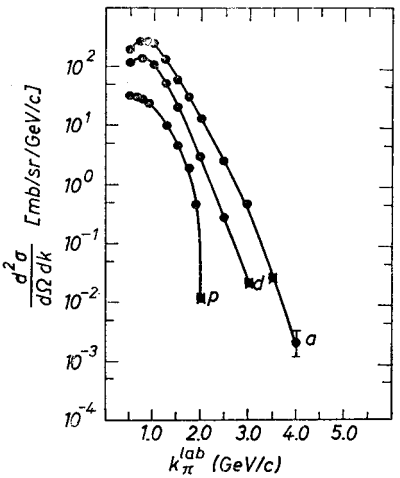

Fig. 15. Laboratory cross section ($d^2\sigma/d\Omega dk$) for π^- production (Ref. [13]) at 2.5° (Lab) for 2.1 GeV/nucleon p, d, α on carbon target versus pion momentum

fied calculation was performed in which the pions were assumed to be produced in an individual nucleon-nucleus collision with Fermi motion included. The form of the single pion production cross section in this model is:

$$\sigma^{\pi}_{aA}(\vec{p}_a, \vec{k}_\pi) = \sum_{N}^{a} \int W_{aN}(\vec{p}_a, \vec{p}_N)\sigma^{\pi}_{NA}(\vec{p}_N, \vec{k}_\pi)d^3p_N, \tag{3}$$

where W_{aN} = momentum distribution of a nucleon in the projectile appropriately transformed to the laboratory frame, σ^{π}_{NA} are measured nucleon-nucleus pion production cross sections (theoreby taking into account the Fermi motion in the target). The model assumed charge symmetry ($\sigma^{\pi^+}_{pC} = \sigma^{\pi^-}_{nC}$) to obtain neutron-induced cross sections from carbon; and to correct for the fact that production was a fixed laboratory angle, the measured cross sections were folded with $\exp[-5|k_\pi| \sin(\theta_{k\pi} - \theta_{pN})]$. Figure 16 shows the results (solid curves) of this calculation for pion production by deuterons and alphas at 1.05 and 2.1 GeV/nucleon. The general behavior of the measured cross sections for fast pions is reproduced quite well. There were no free parameters involved in th calculation. These results disagree with the conclusions of the Dubna group [15], who claim to be unable to fit their data with a similar model. Their calculations indicate that only about 10% of their cross section can be accounted for by Fermi motion and they invoke a collective mechanism for the remainder of the cross sections. It should be pointed out

that for the case of production by deuterons, one cannot distinguish between a Fermi motion model and collective effects, because they amount to the same thing; that is, high Fermi momentum components necessarily imply that the two nucleons in the deuteron are spatially close together and therefore correlated. This suggests that pion production by heavier projectiles (carbon or heavier) would be a better choice for comparing the two mechanisms (Fermi motion vs collective effect) since a large Fermi momentum for a single

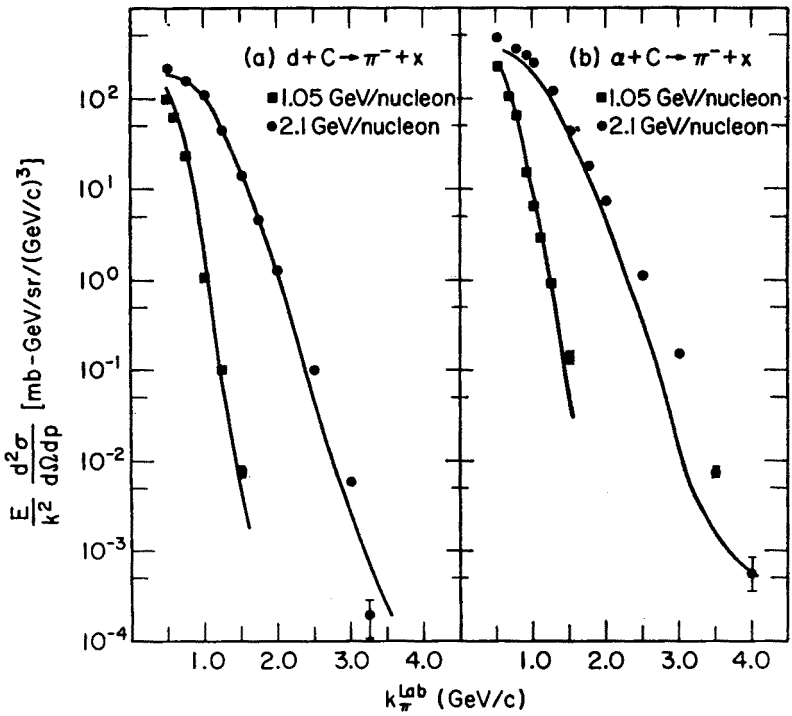

Fig. 16. Invariant cross section for negative pion production at 2.5° (Lab) at 1.05 and 2.1 GeV/nucleon by (a) deuteron and (b) alpha beams. Solid line represents the prediction of model described in Ref. [13]

bound nucleon would not imply as much correlation with other nucleons as is present in the case of the deuteron. Measurements of very high energy pion production by heavier projectiles is presently underway at Berkeley [16].

Additional information on the production mechanism for pions can be obtained by studying the dependence of the production cross section on target mass. As before [12], the production has been parameterized in the form: $\sigma \propto A^n$, where A is the mass of the target. A plot of n as a function of pion momentum for 2.1 GeV/nucleon alphas is shown in Fig. 17. For momenta $\gtrsim 1$ GeV/c the dependence of $A^{1/3}$ suggests peripheral production. For lower momentum pions, the dependence is more pronounced, suggesting that slow pions are produced in more central collisions. A similar effect is seen at the lower energy (1.05 GeV/nucleon) and in the deuteron data [13].

For isospin-zero nuclei like deuterons, alphas and carbon charge symmetry predicts that in reactions like $dC \to \pi^{\pm} + x$ the π^+/π^- ratio should be unity. This has been tested and found to be good to the level of $\pm 10\%$ in these data [13] for deuterons and alphas. More accurate experiments will be required to test this further.

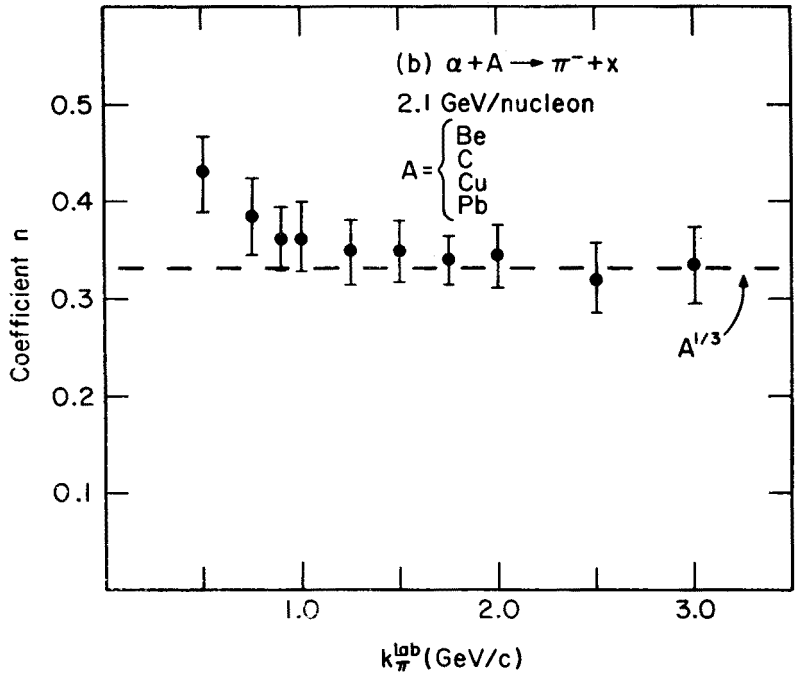

Fig. 17. Dependence of pion production on A. Cross section assumed to have the form: $\sigma \propto A^n$, A = target mass

C) Nucleus-Nucleus Total Cross Section Measurements: Jaros et al. [17] have made systematic measurements of nucleus-nucleus total cross sections for the following target/projectile combinations at 0.87 and 2.1 GeV/nucleon:

projectile \ target	p	d	α	C
p	pp	pd	pα	pC
d	dp	dd	dα	dC
α	αp	αd	αα	αC
C	Cp	Cd	Cα	CC

Note that if the kinetic energy/nucleon of the projectile is fixed, and if we neglect nuclear binding energy, then intercharging target and projectile will cause no change in the center-of-mass energy. Therefore the total cross section, σ_T, will be the same; independent of whether A is the projectile and B the target, or vice versa.

Glauber multiple scattering theory [18] has been used to accurately predict nucleon--nucleus total cross sections in the few GeV range. The formalism involves the folding of the basic nucleon-nucleon scattering amplitudes with the known nuclear matter distribution. The theory has been extended to nucleus-nucleus collisions [19] and used to predict total and inelastic cross sections. The theory is essentially geometrical and predicts that, $\sigma_T \propto (A_{\text{target}}^{1/3} + A_{\text{projectile}}^{1/3})^2$. One of the primary purposes of these measurements was to provide measurements which could be compared to the theory.

In addition, an observation by Gribov [20] also provided stimulus for this experiment. He noted that if one naively applied Regge factorization to nucleus-nucleus collisions it would lead to a very different A-dependence for σ_T than that expected from geometrical considerations. If one assumes factorization and Pomeron dominance, then we can write that the elastic scattering amplitude, $F_{el} \propto g_{PA} g_{PB}$, where the g's refer to the appropriate vertex-Pomeron coupling constants for nucleus A colliding with B. Using the optical theorem, which relates the imaginary part of the elastic amplitude to σ_T, one arrives at the relationship:

$$\sigma_T(AA) = \frac{\sigma_T^2(AB)}{\sigma_T^2(BB)} . \tag{4}$$

If we let B = nucleon = p, and use fact that $\sigma_T(pA) \propto A^{2/3}$, we obtain:

$$\sigma_T(AA) \propto A^{4/3}. \tag{5}$$

Thus, factorization predicts $A^{4/3}$, while a Glauber approach would predict $A^{2/3}$, quite different and easily testable.

The "good geometry" transmission technique [21] was used to make these measurements. The technique consists of measuring the beam particles which are scattered by the target with a set of circular counters of increasing size. In this way, one can extrapolate the measurements to zero solid angle. There are two contributions to the scattering process at small angles; coulomb and nuclear scattering. With nuclear beams and targets, the coulomb amplitude will necessarily play a larger role. The separation of the coulomb and nuclear effects are major theoretical and experimental problems.

Fig. 18 shows the results of these measurements at 2.1 GeV/nucleon. The solid and dashed curves are the predictions of Glauber theory and the factorization relation, respectively. The data is seen to be in excellent agreement with the Glauber prediction for all data points except the CC point which lies slightly below the Glauber theory prediction. The fact that the factorization prediction is not satisfied could be anticipated, since it is only supposed to be valid at energies much larger than those available in this experiment.

D) Nuclear γ-Ray Production: The TOSABE group [22] has been investigating γ-ray production from peripheral nucleus-nucleus collisions. Their motivation lies in the fact that by observing discrete lines, they hope to select very peripheral interactions. By studying photons from known spin-parity and isospin states they may obtain more information on the transferred angular momentum in these collisions. Further, by identify-

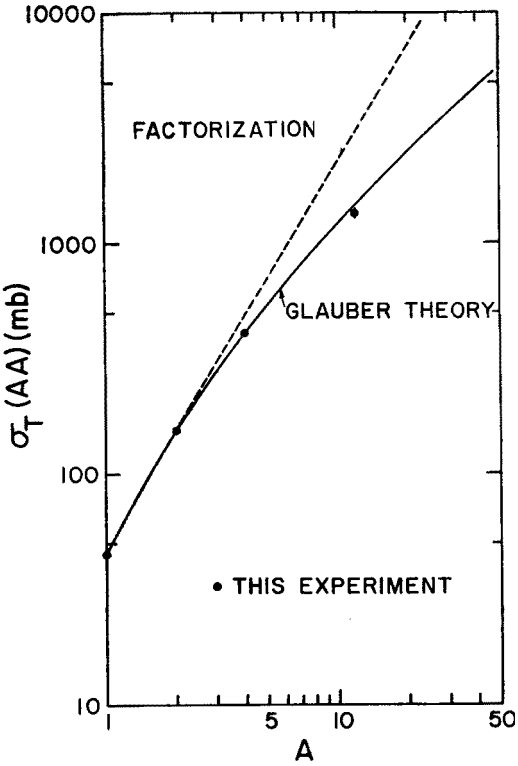

Fig. 18. Measured total cross sections ($\sigma_T(AA)$) compared with predications of factorization and Glauber models. Data taken at 2.1 GeV/nucleon

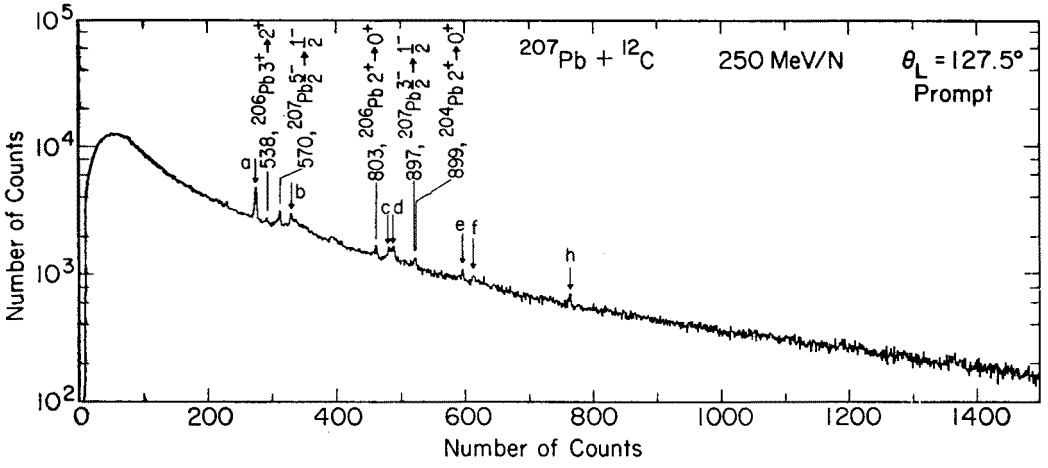

Fig. 19. Example of γ-ray spectrum produced at 127.5° (Lab) by 250 MeV/nucleon carbon ions on ^{207}Pb. Known lines are indicated. Lines referred to by small letter designation are due to material in vicinity of target area

ing the residual nucleus through the detection of well known levels, one can obtain information on reaction mechanisms, such as nucleon or alpha knock-out, and neutron evaporation. Thus, their study can contribute significant information on the dynamics of the nucleus-nucleus interaction.

The experiments were performed using carbon projectiles at 250 MeV/nucleon and 1.05 GeV/nucleon on a variety of targets (^{12}C, ^{19}F, Sr, ^{207}Pb). Fig 19 shows a sample spectrum for a ^{207}Pb target (known lines are indicated). It is worth noting the large background under the known lines. A portion of this background, which is of a "bremstrahlung nature", could be assosiated with more central collisions. Cross sections for the lines that are identified are typically in the range of 10–100 mb. There are early indications in these measurements that high spin states of the target are excited in these collisions [22]. This is not observed in experiments at much lower energies ($\sim$ 10 MeV/nucleon). This work has just scratched the surface, and a long term program on γ-ray detection is developing.

To summarize the discussion on peripheral collisions, we see that a large bulk of the total nucleus-nucleus reaction cross section appears in peripheral collisions. Included in this category are the phenomena of projectile fragmentation, and a portion of pion and γ-ray production. Experiments to-date have been almost exclusively of the single-particle inclusive type. Theoretical calculations are just now starting to be refined enough to aid in explaining some of the observed features of peripheral interactions. Much work, both theoretical and experimental remains to be done. In particular, the next experimental step will involve correlation studies, calling for the detection of two or more particles in the final state.

3. Central collisions

We now turn our attention from the area of peripheral collisions to a consideration of collisions where there is a substantial overlap of nuclear material in the projectile and target nuclei. One of the interesting questions that has arisen in studies of high energy nucleus-nucleus collisions is whether energetic nuclei can deposit more energy and momentum in a target nucleus than other forms of hadronic probes such as pions or nucleons. Zebelman et al. [23] have recently mesured the energy and angular distributions of fragments (He to B) produced by 4.9 GeV protons and 2.1 GeV/nucleon deuterons and alphas striking a uranium target. Relative cross sections for the production of ^{4}He and ^{7}Li fragments at 90° in the laboratory plotted against the kinetic energy of the fragment are shown in Fig. 20. Also included in Fig. 20 are more recent data [24] from 2.1 GeV/nucleon ^{12}C and ^{20}Ne runs. From these data we see that incident deuterons do not appear to produce significantly more fragments than do high energy protons. However, in the interaction of α, C, and Ne with uranium there is a definite indication of larger fragment yields, suggesting a larger deposition energy. Thus, high energy nuclei perhaps provide a more effective tool for depositing large amounts of energy and momentum in a nucleus. What happens to this deposite energy and momentum serves as the basis for the remainder of this talk.

Under what conditions would we expect large energy and momentum depositions to occur? What experimental signatures might arise that would allow us to selectively study these particular processes? Certainly, if two nuclei collide in a central fashion there is a large overlap of nuclear matter. The probability for interaction would be increased for this condition, and one expects that these events present the best change for depositing

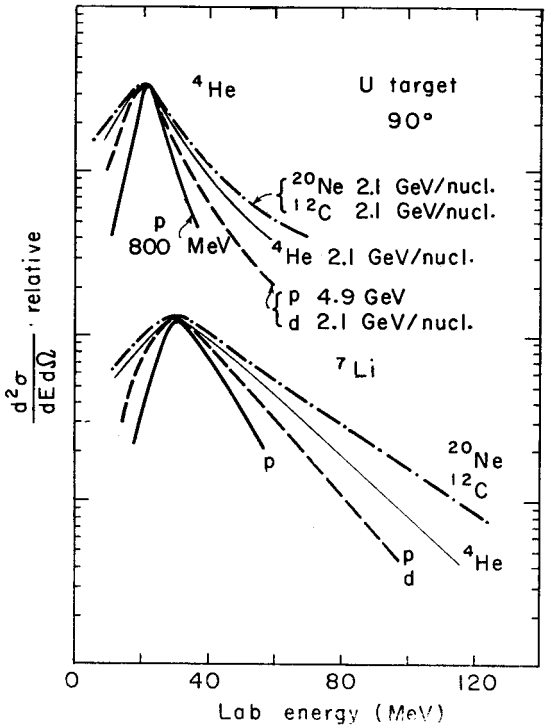

Fig. 20. Relative cross sections (Ref. [23–24]) for the production of ^{4}He and ^{7}Li fragments at 90° in the lab from a uranium target bombarded by various energy p, d, α, C, and Ne beams

large amounts of energy and momentum. For a central collision, where the nuclei are not transparent to each other, we would expect that the deposited energy and momentum would go into liberating large numbers of particles. So a large multiplicity of particles acts as one possible signature for a central collision [25]. An illustration of this is seen in Figure 21, which shows the collision of a 1.8 GeV/nucleon ^{40}Ar nucleus with a lead--oxide target located inside the LBL streamer chamber [3]. In this spectacular event, a large number of positive and negative charged particles were produced over the whole solid angle, with no large mass remnants of the projectile appearing from the interaction. This should be contrasted to the picture showing projectile fragmentation (Fig. 2), where all the particles were produced in a very small solid angle about the beam direction.

There has recently been a good deal of theoretical interest in heavy ion collisions at high energies. The most exciting speculations have involved the possibility of observing new phenomena associated with the central collisions of these energetic nuclei. Included

among these are: abnormal nuclei [26], highly excited nuclear matter [27], nuclear shock waves [28], and pion condensates [29]. These speculations have been greeted by intense experimental activity which I now want to review. This review will include: search for shock waves in nuclear matter and studies of particle multiplicities using the streamer chamber.

A) Search for Shock Waves in Nuclei: In 1959 Glassgold et al. [30] suggested that shock waves might be sent-up in a nucleus by the passage of a high energy nucleon. This speculation remained somewhat dormant for a number of years. Recently [28, 31, 32] predictions of nulear shock waves carrying large amounts of transverse energy and momentum have been put forth. It has been suggested that shock waves might be produced in the central collision of two nuclei when the projectile velocity exceeds the nuclear sound velocity, $v \approx 0.2\ c$. If a shock wave produced and propagated through the nuclear medium, upon impacting the surface it would eject particles. These particles would be numerous and have energies $\gtrsim$ 10–20 MeV/nucleon. Some predictions [33] suggest that particle emission by these shock waves will occur in a narrow band ($\sim$ 20–45°) of angles. This angular band would move to backward angles as the projectile energy is increased (an experimental feature to look for). A hydrodynamic model [32] suggested that the angular range for emission would be larger. A possible key to the detection of nuclear shock waves would be the presence of peaks in the angular distribution of light nuclear fragments.

One of the first experiments to produce results on shock waves was the Frankfurt group [33] using Ag-Cl detectors exposed to carbon and oxygen beams. The technique used was to optically scan the processed Ag-Cl detectors for recoil tracks. No particle identification is made, but the detectors are sensitive to protons less than 28 MeV ($\beta \approx 0.24$) and He nuclei less than 200 MeV/nucleon ($\beta \approx 0.57$). To select central collisions, they choose only so-called "star events"; those exhibiting a large number of prongs. After this event selection, they observed peaks in the angular distribution ($N(\theta) = d\sigma/d\theta$) of fragments at several projectile energies and conclude that the particles in their angular distributions were dominately due to protons and He nuclei. Fig. 22 shows their angular distributions, for "star events", from ^{16}O and ^{12}C bombardment of their detector. Note that they plot $d\sigma/d\theta$ rather than $d\sigma/d\Omega$ ($d\sigma/d\theta = 2\pi \sin\theta\,(d\sigma/d\Omega)$). In each of the angular distributions a relatively narrow peak ($\approx$ 20–40°) is present, which shifts to backward angles with increasing projectile energy. The solid curve represents their estimate of particles evaporated from the target (a background process to the shock wave phenomena). Using these [33] and later data [34], they conclude that they have positive evidence for nuclear shock wave.

In an effort to study the possibility of shock wave emission of light nuclear fragments with larger statistics, Poskanzer et al. [24] in a single particle inclusive counter experiment (solid state detectors using E-ΔE techniques, in conjunction with a scintillator counter) measured the energy ($E \lesssim 50$ MeV/n) and angular distribution of ^3He and ^4He fragments from silver and uranium targets bombarded by protons, alphas and ^{16}O ions. Figure 23 shows their angular distribution ($d\sigma/d\Omega$) for ^3He and ^4He fragments with energy cuts to simulate as closely as possible the conditions of the Ag-Cl experiment [33]. These

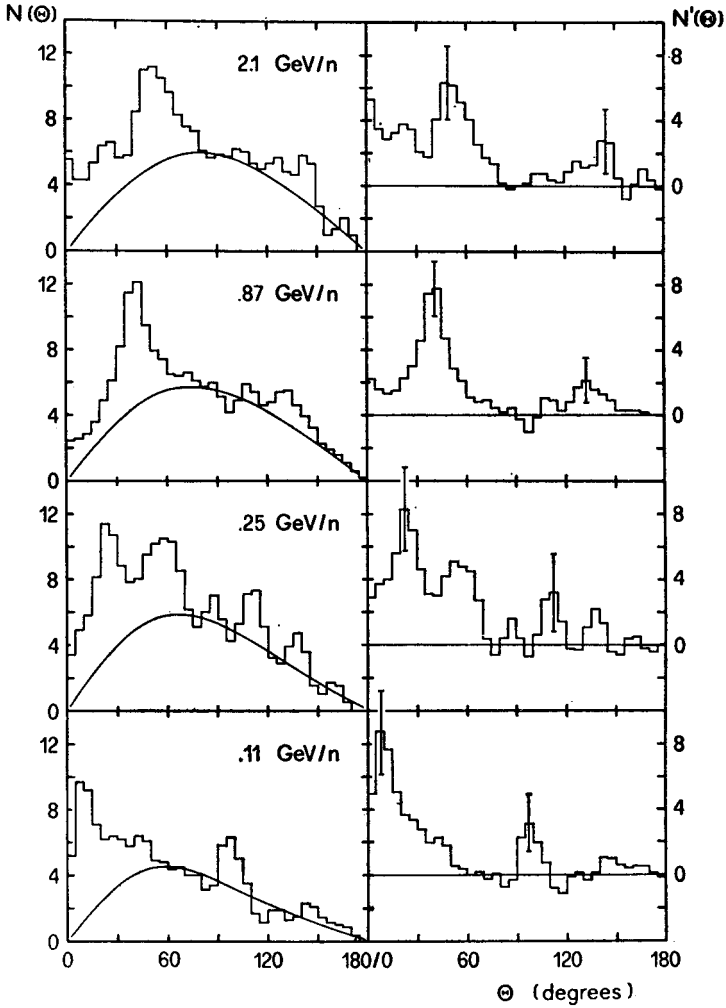

Fig. 22. Data from Ref. [23]. Left-hand column contains their angular distributions requiring a large multiplicity of prongs. Right-hand column contains angular distributions after background subfraction. 2.1 and 0.87 GeV/n data are for ^{16}O projectiles, 0.25 and 0.11 GeV/n data are for ^{12}C projectiles

distributions are seen to be smoothly varying. No narrow peaks are seen in either of this angular distribution or the one shown in Fig. 24 where the data is plotted as $d\sigma/d\theta$ to compare with the Ag–Cl experiment. This experiment attempted to reproduce as closely as possible the experimental conditions of the Ag–Cl work, but had no multiplicity capability. Presently an experiment is underway which includes the capability of measuring multiplicities associated with single fragments registering in their detector system.

In an emulsion experiment, Otterlund et al. [35] have looked for evidence of shock waves produced by 0.2 and 2.0 GeV/nucleon ^{16}O ions. They have made cuts on charged particles with energy loss greater than that expected for an 11 MeV proton. They have observed no statistically significant narrow peaks in their angular distributions.

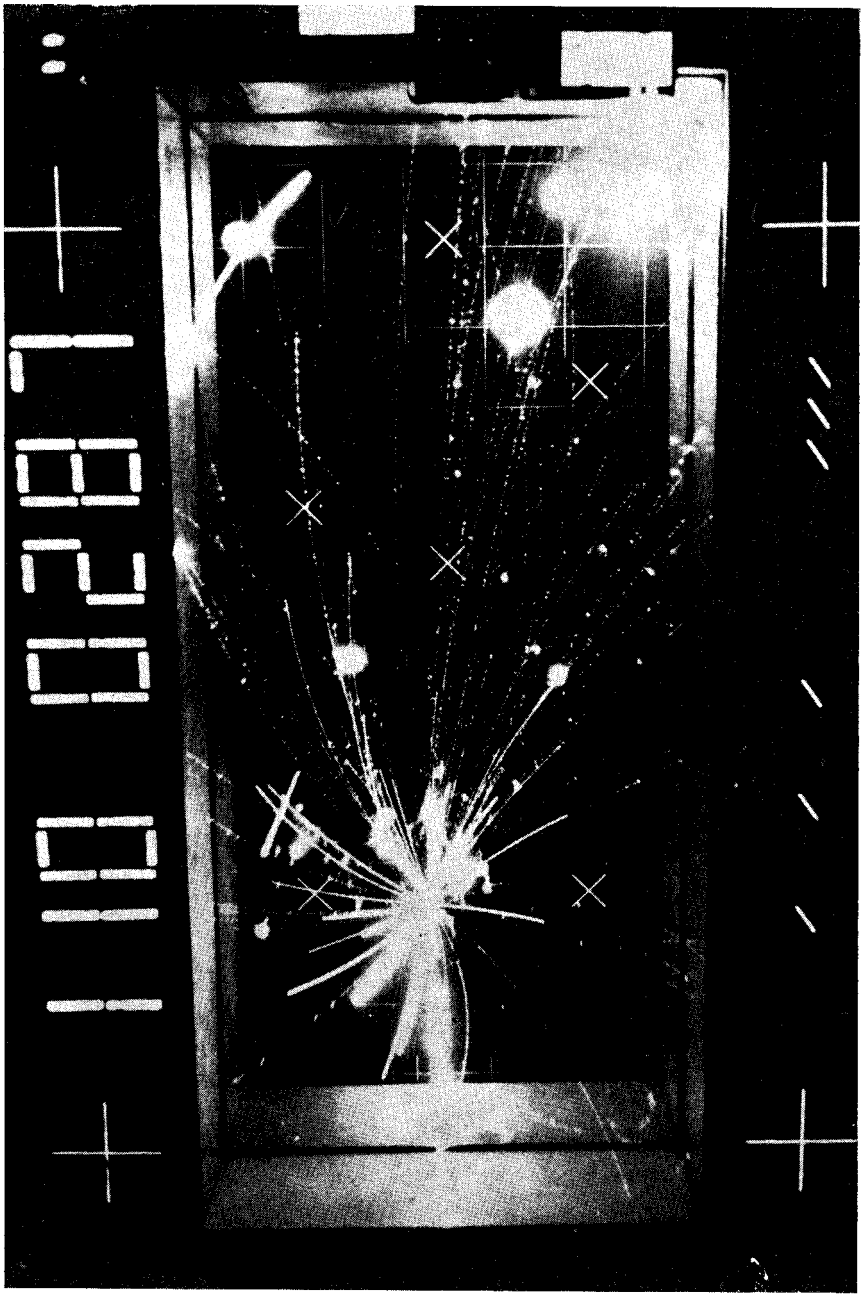

Fig. 21. 1.8 GeV/nucleon ^{40}Ar projectile interacting with a thin Pb_3O_4 target inside LBL streamer chamber. Positive particles bend down in magnetic field of chamber, and negative particles bend up

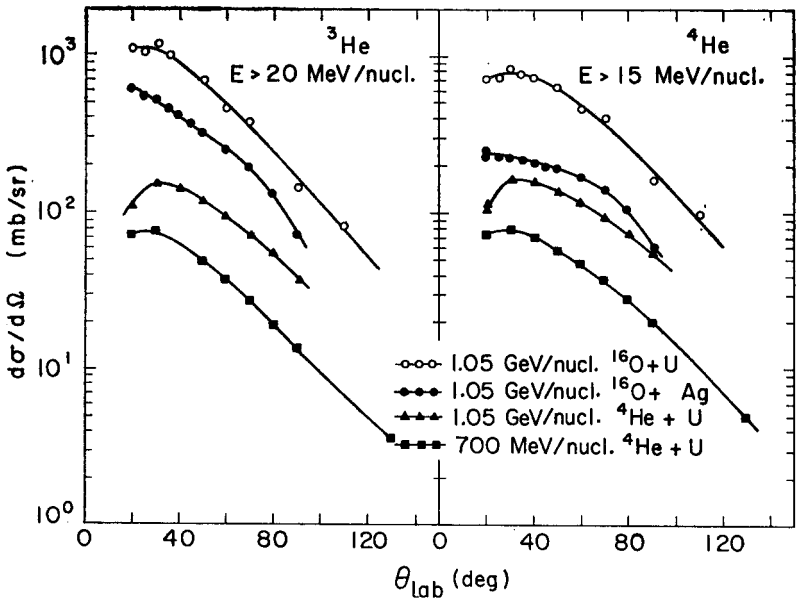

Fig. 23. Angular distributions of ^{3}He and ^{4}He fragments obtained by bombarding Ag and U targets with ^{4}He and ^{16}O projectiles

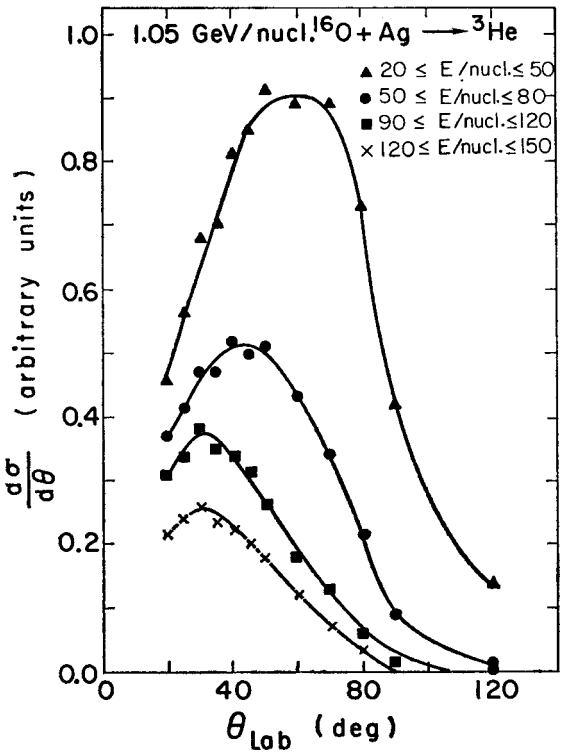

Fig. 24. Differential cross sections unit angle, $d\sigma/d\theta$, of He fragments emitted in various energy windows between 20 and 150 MeV/n from ^{16}O on Ag collisions at 1.05 GeV/n

At present, there does not appear to be any overwhelming evidence for the existence of nuclear shock waves. On the one hand, the Frankfurt group observes narrow peaks (for high multiplicity events), but needs to greatly improve their statistics, as well as demonstrating that their detector sensitivity does not introduce unwanted biases. The high statistics experiment of Poskanzer et al. [24] measuring only the single particle angular distribution, observes no peaks; but has no multiplicity cuts which can help to select central collisions. Emulsion work [35], where multiplicity cuts can be made, observes no peaks, but could use an improvement in statistics.

B) Streamer Chamber Experiments — An Early Look: Except for a few detectors like emulsions or the Ag–Cl detectors of the Frankfurt group, visual techniques have not been used to study high energy nuclear collisions at the Bevalac. Recently, the LBL streamer chamber has been put to work studying nucleus-nucleus collisions by a U.C. Riverside/LBL collaboration [3]. The streamer chamber is a large gas filled volume

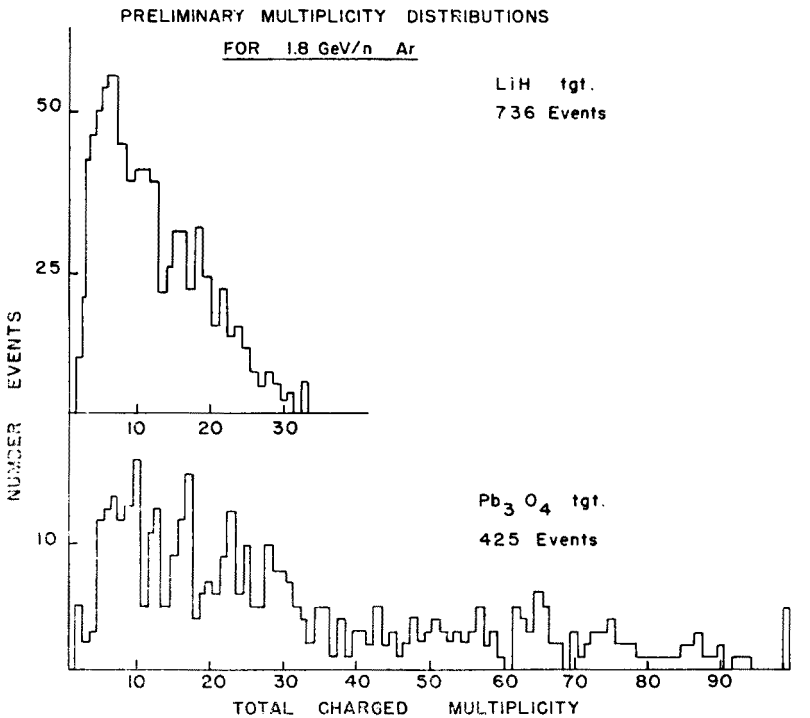

Fig. 25. Preliminary multiplicity distributions for positive and negative fragments produced by 1.8 GeV/n ^{40}Ar projectile on LiH (upper graph) and Pb_3O_4 (low graph) terget

(1.1 m × 0.6 m × 0.3 m) which is placed in a large magnetic field. Charged particles traversing the gas of the chamber produce ionization; a high voltage pulse (15 nanoseconds in duration and 500–750 k volts) when applied causes a series of streamers to develop. These streamers are photographed and indicate the path of the charge particle through

the gas. Thus, the streamer chamber is a unique tool which provides $\sim 4\pi$ geometry for detection and with the ability to be selectively triggered by electronic counters located either inside or outside the chamber. In this experiment, four non-conducting targets (LiH, NaF, BaI_2, Pb_3O_4) were placed in the chamber and exposed to a beam of 1.8 GeV/nucleon Ar nuclei. One of these interactions resulted in the spectacular event shown in Fig. 21. It is worth noting that in this particular event, the incident Ar nucleus appears to have been reduced to its basic constituents (nucleons and perhaps other light fragments). Large numbers of particles are seen at all angles, indicating that a large amount of energy and momentum can be transferred in these collisions. Also note the absence of any large fragments of the projectile in the forward direction.

An additional piece of information becomes readily apparent when scanning Fig. 21; namely, the task of extracting all the information available in such pictures is enormous. Pictures with up to 125 charge tracks have been found. It is too much to expect that one could measure (with high efficiency) that many tracks in a single event. So how does one go about obtaining information from these pictures? First, a simple scanning of the film will reveal the multiplicity for charged particles. Figure 25 shows preliminary multiplicity distributions for light and heavy targets. From these it is evident that there is a large cross section for high multiplicity events with the heavy target. The broad peak appearing at lower multiplicities can be associated with projectile fragmentation processes. Additional things to study are: negative tracks, which are presumably π^-'s (up to 15 have been observed in a single event), emission of light fragments at backward angles and correlations between various tracks. In the near future, additional exposures will be made so that a series of systematic studies (as a function of projectile mass and energy for both light and heavy targets) will exist.

The studies of phenomena which arise as a result of the head-on collision of two nuclei will be playing a larger and larger role at the Bevalac. In these collisions, new and exotic states of nuclear matter might be found.

4. Future developments

Two major improvements are presently planned which will substantially extend the capabilities of the Bevalac to explore the regime of nucleus-nucleus collisions at high energy. The first modification consists of the installation of a new liner inside the Bevatron's present vacuum chamber. This will improve the pressure from its present level of 5×10^{-7} torr to around 10^{-9} torr. This reduction in pressure will allow the acceleration of much heavier ions. In addition, by accelerating lower charge states of a given ion, this will allow experimental programs with beam energies as low as 50 MeV/nucleon. A third injector added to the SuperHILAC will be required to obtain heavier beams (up to Pb or U). Figure 26 compares the capabilities of the present facility (SuperHILAC and Bevalac) with those of the proposed facility. It is hoped that funding for this project will become available by FY 1978, with operation by FY 1980. These new facilities will not require any major stoppage of the nuclear science programs at either machine.

An additional request has also been made for the funding of a new Heavy Ion Spectro-

meter System (HISS) [36]. HISS features a large solid angle, large magnetic volume, with good energy and spatial resolution. The proposal calls for a superconducting dipole (~ 2 meter diameter, and up to a meter gap) and quadrupoles. A central justification for

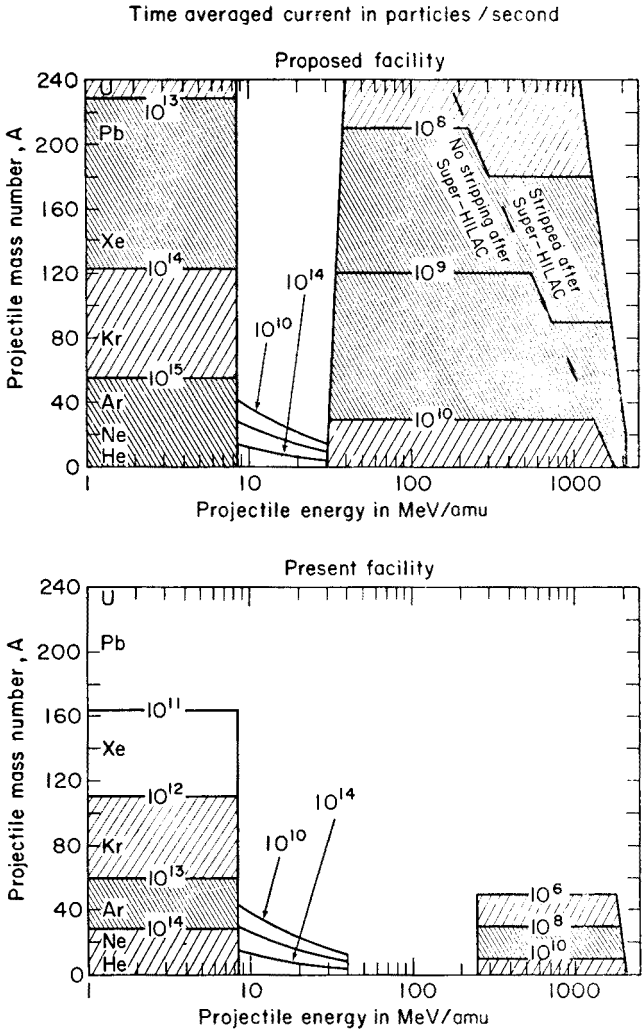

Fig. 26. Comparison of the present (lower graph) and future (upper graph) capabilities of the SuperHILAC and Bevalac in terms of projectile mass and energy

HISS lies in the fact that it will serve as a basic facility for carrying out new generations of physics experiments at the Bevalac. It is designed to operate with heavy-ion beams of 250 MeV/nucleon to 2.1 GeV/nucleon and typical resolutions of $\Delta p/p \sim 10^{-3}$. If approved, it is hoped that construction would begin by 1978, with approximately a two year construction period before completion and operation.

5. *Concluding remarks*

The early stages of nucleus-nucleus studies at high energies have been of a survey nature. Single-particle inclusive studies have led the way in the study of peripheral, and to a large extent, the area of central collisions. Often, only the grossest features of these interactions have been investitgated (e. g., momentum distributions). Now that the period of initial survey is largely behind us, second and third generation experiments will start to look for correlations between fragments and will provide data which can unravel some of the dynamics of processes such as projectile fragmentation. The evolution of the experimental program at the Bevalac Facility is akin to explorers charting unknown lands. First one outlines the gross features such as mountains, rivers and valleys. From there one can then proceed with greater assurance to explore the areas in the mountains and valleys which appear particularly interesting.

The area where the Bevalac will probably make its most profound impact is in the possibility of creating new nuclear phenomena such as shock waves, pion condensates, or abnormal nuclear matter in head-on collisions. Prof. T. D. Lee [37] has pointed out that particle physicists for years have been putting larger and larger energies into smaller and smaller volumes. Using high energy nuclear beams provides us with the first opportunity to put a large energy into a large volume (the nucleus), with the possibility of exciting new consequences.

I wish to thank our Polish hosts at this 1976 Cracow School for their wonderful organization and friendship. In particular, my thanks go to Drs. A. Białas and W. Czyż and their remarkable wives for this oportunity to lecture at the school and to learn from the other students and lecturers.

REFERENCES

[1] *Cern Courier*, No. 4, Vol. 16, Appril 1976, p. 134.

[2] For other reviews on high energy nucleus-nucleus work at Berkeley see: H. Steiner, *Particle Production by Relativistic Heavy Ions*, *Proceedings on High Energy Collisions Involving Nuclei*, Trieste, Italy 1974, eds. G. Bellini, L. Bertocchi, P. G. Rancoita, Editrice Compositori — Bologna, p. 151–170; B. Cork, *Fragmentation of Relativistic Nuclei*, AIP Conference Proceedings No. 26, High Energy Physics and Nuclear Structure, eds. D. Nagle, A. Goldhaber, C. Hargrove, R. Burman and B. Storms, Santa Fe and Los Alamos 1975, p. 598–620.

[3] S. Fung, B. Gorn, A. Kernan, G. Kiernan, J. Lu, Y. Oh, J. Ozawa, R. Poe, B. Shen, G. Van Dalin (U. C. Riverside), L. Schroeder, H. Steiner (LBL), Experiment 228H at the Bevalac Facility, *Studies of Particle Production and Fragmentation in the LBL Streamer Chamber.*

[4] H. H. Heckman, D. E. Greiner, P. J. Lindstrom, F. S. Bieser, *Phys. Rev. Lett.* **28**, 926 (1972); D. E. Greiner, P. J. Lindstrom, H. H. Heckman, B. Cork, F. S. Bieser, *Phys. Rev. Lett.* **35**, 152 (1975).

[5] J. V. Lapore, R. J. Riddell, Jr., LBL-3086, 1974.

[6] W. A. Wenzel, *LBL Heavy Ion Seminar* at LBL (unpublished 1973).

[7] H. Feshbach, K. Huang, *Phys. Lett.* **47B**, 300 (1973).

[8] A. S. Goldhaber, *Phys. Lett.* **53B**, 306 (1974).

[9] J. Hüfner, K. Schafer, B. Shurmann, *Phys. Rev.* **C12**, 1888 (1975); A. Abul-Magd, J. Hüfner B. Shurmann, preprint submitted to *Phys. Lett.* B (1976); A. Abul-Magd, J. Hüfner, Univ. of Heidelberg, preprint 1976.

[10] J. D. Bowman, W. J. Swiatecki, C. F. Tsang (LBL), unpublished 1973.
[11] H. H. Heckman, P. J. Lindstrom, LBL-4380, 1976.
[12] J. Papp, *Single Particle Inclusive Spectra Resulting from the Collision of Relativistic Protons, Deuterons, Alpha Particles and Carbon Ions with Nuclei*, LBL-3633, 1975.
[13] J. Papp, J. Jaros, L. Schroeder, J. Staples, H. Steiner, A. Wagner, J. Wiss, *Phys. Rev. Lett.* **34**, 601 (1975).
[14] R. P. Feynmann, *Phys. Rev. Lett.* **23**, 1415 (1969).
[15] A. M. Baldin, S. B. Ferasimov, M. Guiordenseu, V. N. Zubarev, L. K. Ivanova, A. D. Kirillov, V. N. Kuznetsov, N. S. Moroz, V. D. Radomanov, V. N. Ramzhin, V. S. Stavinskii, M. Yatsuta, *Yad. Fiz.* **18**, 79 (1973) (*Sov. J. Nucl. Phys.* **18**, 41 (1974)).
[16] L. Anderson, O. Chamberlain, D. Nygren, S. Nagamiya, S. Nissen-Meyer, G. Shapiro, L. Schroeder, H. Steiner, Expt. 205H, *Pion Production and Fragmentation Studies with High Energy p, d, α, and C Ions.*
[17] J. Jaros, L. Anderson, O. Chamberlain, R. Fuzesy, J. Gallup, W. Gorn, L. Schroeder, S. Shannon, G. Shapiro, H. Steiner, A. Wagner, J. Wiss, Expt. 170H, *Heavy Ion Total Cross Section* and J. Jaros, LBL-3849, 1975 (unpublished thesis).
[18] R. J. Glauber in *Lectures in Theoretical Physics*, Vol. 1, Interscience, New York 1959, p. 315; R. J. Glauber in *High Energy Physics and Nuclear Structure*, North-Holland, Amsterdam 1967, p. 311; R. J. Glauber in *High Energy Physics and Nuclear Science*, North-Holland, Amsterdam 1969, p. 207.
[19] W. Czyż, L. C. Maximon, *Ann. Phys.* (New York) **52**, 59 (1969).
[20] V. N. Gribov, *Sov. J. Nucl. Phys.* **9**, 369 (1969).
[21] G. Giacomelli in *Progress in Nuclear Physics*, Vol. 12, Pergamon Press, New York 1970, p. 77.
[22] TOSABE stands for a collaboration of the Univ. of Tokyo, Osaka University, and Berkeley. H. Ejiri, T. Shibata, R. Anholt, H. Bowman, J. G. Iounnon-Yannon, J. O. Rasmussen, E. Rausher, S. Nagamiya, K. Nakai, *Nuclear Gamma Rays Following Interaction with Relativistic Carbon Projectiles*, LBL-5056, 1976.
[23] A. M. Zebelman, A. M. Poskanzer, J. D. Bowman, R. G. Sextro, V. E. Viola, Jr., *Phys. Rev.* **C11**, 1280 (1975).
[24] A. M. Poskanzer, R. G. Sextro, A. M. Zebelman, H. M. Gutbrod, A. Sandoval, R. Stock, *Phys. Rev. Lett.* **35**, 1701 (1975).
[25] There are other approaches being used besides large multiplicity to bias experiments towards central collisions. One of these, *Measurements of Transverse Momenta of Fragments Emitted after Nuclei-Nucleus Head-On Collisions*, S. Nagamiya, L. Anderson, O. Chamberlain, G. Shapiro, H. Steiner, Expt. 299H, will be looking for the azimuthally symmetric production of fragments to signal a central collision.
[26] T. D. Lee, G. C. Wick, *Phys. Rev.* **D9**, 2291 (1974), and *Abnormal Nuclear States and Vacuum Excitation, Proceedings of the Topical Meeting on High-Energy Collisions Involving Nuclear*, Trieste, Italy 1974, G. Bellini, L. Bertocchi, P. G. Rancoita, eds. (Editrice Compositori, Trieste 1974), p. 247–270.
[27] G. Chapline, M. Johnson, E. Teller, M. Weiss, *Phys. Rev.* **D8**, 4302 (1973); and the *Proceedings of the 2nd High Energy Heavy Ion Summer Study*, Berkeley 1974, Lawrence Berkeley Laboratory, LBL-3675, p. 51–71.
[28] W. Scheid, H. Muller, W. Greiner, *Phys. Rev. Lett.* **32**, 741 (1974); and p. 1–50 of the *Proceedings of the 2nd High Energy Heavy Ion Summer Study*, 1974 at the Lawrence Berkeley Laboratory, LBL-3675.
[29] A. B. Migdal, *π-Condensation of Abnormal Nuclei, Proceedings of the High Energy Physics and Nuclear Structure Conference*, eds. D. E. Nagle, A. S. Goldhaber, C. K. Hargrove, R. L. Burman, B. G. Storms. Santa Fe and Los Alamos 1975. AIP Conference Proceedings No. 26,
[30] A. E. Glassgold, W. Heckrotte, K. M. Watson, *Ann. Phys.* (New York) **6**, 1 (1959).
[31] C. Y. Wong, T. A. Welton, *Phys. Lett.* **49B**, 243 (1974).
[32] A. A. Amsden, G. F. Bertsch, F. H. Harlow, J. R. Nix, *Phys. Rev. Lett.* **35**, 905 (1975).
[33] H. G. Baumgardt, J. U. Schott, E. Schopper, H. Stocker, J. Hofman, W. Schied, W. Greiner, *Z. Phys.* **A273**, 359 (1975).

[34] H. G. Baumgardt, E. Schopper, J. V. Schott, N. P. Kocherov, A. V. Veronov, I. D. Issinsky, L. G. Markarov, *Proceedings of the International Work-shop on Gross Properties of Nuclei and Nuclear Excitation IV*, Hischegg 1976 Kleinwadsertal, Austria, 1976, p. 105–110.

[35] B. Jakobsson, R. Kullberg, I. Otterlund, *Search for Shock Wave Phenomena in Central ^{16}O–AgBr Interactions at 0.2 and 2.0 GeV/nucleon*, University of Lund preprint 1976; I. Otterlund, private communication.

[36] P. Lindstrom, J. Carroll, H. Heckman, D. Hendrie, L. Schroeder, LBL–5013.

[37] T. D. Lee, invited talk at 1974 Bevatron User's Meeting, January 1974, LBL.